



저작자표시-비영리-변경금지 2.0 대한민국

이용자는 아래의 조건을 따르는 경우에 한하여 자유롭게

- 이 저작물을 복제, 배포, 전송, 전시, 공연 및 방송할 수 있습니다.

다음과 같은 조건을 따라야 합니다:



저작자표시. 귀하는 원저작자를 표시하여야 합니다.



비영리. 귀하는 이 저작물을 영리 목적으로 이용할 수 없습니다.



변경금지. 귀하는 이 저작물을 개작, 변형 또는 가공할 수 없습니다.

- 귀하는, 이 저작물의 재이용이나 배포의 경우, 이 저작물에 적용된 이용허락조건을 명확하게 나타내어야 합니다.
- 저작권자로부터 별도의 허가를 받으면 이러한 조건들은 적용되지 않습니다.

저작권법에 따른 이용자의 권리는 위의 내용에 의하여 영향을 받지 않습니다.

이것은 [이용허락규약\(Legal Code\)](#)을 이해하기 쉽게 요약한 것입니다.

[Disclaimer](#)

의학박사 학위논문

산모의 비스페놀 A(bisphenol A)
노출이 후성유전학적 기전을 통해
소아의 비만에 미치는 영향

Effect of prenatal bisphenol A exposure on
child's obesity through epigenetic mechanism

2021년 2월

서울대학교 대학원
의학과 예방의학 전공
최 윤 정

A thesis of Degree of Doctor of Philosophy

**Effect of prenatal bisphenol A
exposure on child's obesity
through epigenetic mechanism**

**산모의 비스페놀 A(bisphenol A) 노출이
후성유전학적 기전을 통해
소아의 비만에 미치는 영향**

February 2021

Yoon-Jung Choi

Department of Preventive Medicine

Soeul National University College of Medicine

산모의 비스페놀 A(bisphenol A) 노출이 후성유전학적 기전을 통해 소아의 비만에 미치는 영향

지도교수 홍 윤 철

이 논문을 예방의학 박사학위논문으로 제출함

2020년 12월

서울대학교 대학원

의학과 예방의학 전공

최 윤 정

최윤정의 박사학위논문을 인준함

2021년 1월

위원장	박수경	(인)
부위원장	홍윤철	(인)
위원	박상민	(인)
위원	최지엽	(인)
위원	배상혁	(인)

A thesis of Degree of Doctor of Philosophy

**Effect of prenatal bisphenol A
exposure on child's obesity
through epigenetic mechanism**

by

Yoon-Jung Choi, M.D., M.Sc

**A thesis submitted to the Department of
Medicine in partial fulfillment of the
requirements for the Degree of Doctor of
Philosophy in Medicine (Preventive Medicine)
at Seoul National University College of Medicine**

January 2021

Approved by Thesis Committee

Professor Soo K. Park Chairmen

Professor Yungho Jung Vice Charimen

Professor Sang Min Park

Professor Ji-Yeob Choi 조지영

Professor Hyun-Gook Kim

Abstract

Effect of prenatal bisphenol A exposure on child's obesity through epigenetic mechanism

Yoon-Jung Choi

**Department of Preventive Medicine
Seoul National University College of Medicine**

BACKGROUND: *In utero* exposure to bisphenol A (BPA) has been indicated as an obesogen in children, and epigenetic regulations have been suggested as underlying mechanisms with limited evidence in humans.

OBJECTIVES: Differentially methylated CpG sites by prenatal BPA exposure were identified and evaluated for their association with DNA methylation and obesity in children by candidate gene analysis.

METHODS: DNA methylation profiles were investigated in whole blood from 59 children at ages 2 and 6 years longitudinally by Infinium HumanMethylation BeadChip, who are participating in Environment and Development in Children cohort study. Among 594 CpG sites reported from previous obesity-related epigenome-wide association studies, differentially methylated CpG sites by prenatal and postnatal BPA exposure (<80 vs. ≥80 percentile) were identified. Differentially methylated CpG sites were then

tested for the associations with body mass index (BMI) and BMI Z-score at ages 2, 4, 6, and 8 years in linear regression models after adjusting for several covariates.

RESULTS: Methylation at cg19196862, located at the 31st exon of insulin-like growth factor 2 receptor (*IGF2R*) gene, differed by prenatal BPA exposure at age 2 (p-value 0.00030, false discovery rate corrected p-value <0.05) but not at age 6, and was positively associated with BMI Z-score at ages 2, 4, 6, and 8 years old. With 1 standard deviation increase of methylation at cg19196862, BMI Z-score increased by 0.253 (95% confidence interval (CI); 0.050, 0.456), 0.243 (95% CI; 0.030, 0.455), 0.251 (95% CI; 0.030, 0.472), and 0.322 (95% CI; 0.034, 0.610) at ages 2, 4, 6, and 8, respectively. DNA methylation levels at 594 CpG sites at age 2 and 6 were not associated with postnatal exposure to BPA at ages 2, 4, and 6.

CONCLUSION: Prenatal exposure to BPA may influence differential methylation of *IGF2R* at age 2, which could persistently affect BMI in children up to 8 years old. Prenatal exposure to BPA did not affect DNA methylation at age 6, which implies that prenatal BPA exposure may be more influential in earlier childhood. DNA methylation at 594 CpG sites were not different by postnatal exposure to BPA at ages 2, 4, and 6 years, suggesting that prenatal BPA exposure may be more important than postnatal exposure.

KEYWORDS: bisphenol A, prenatal, DNA methylation, epigenetics, obesity, BMI, BMI Z-score

Student ID: 2018-36285

Contents

Introduction	1
Methods	3
Study Participants	3
Data collection	3
DNA methylation assessment	4
Quality control for methylation data	6
Systematic review of literature	6
Selection of candidate CpG sites	11
Covariates	13
Statistical analysis	14
Results	18
General characteristics of participants	18
Differential methylation levels in children at ages 2 and 6 years according to prenatal BPA exposure	26
Differential methylation levels in children at ages 2 and 6 years according to postnatal BPA exposure	36
Methylation status at age 2 years and child's BMI in early childhood	41
Mediation analysis	44
Sensitivity analysis	47
Discussion	51
Conclusion	56
References	57
초록	65
Acknowledgment	86

List of Tables

Table 1. Previous epigenome-wide association studies for the association between methylation and obesity	10
Table 2. General characteristics of the sub-cohort according to prenatal BPA exposure level - parental factors (n=59).	20
Table 3. General characteristics of the sub-cohort according to prenatal BPA exposure level - child factors (n=59).	21
Table 4. General characteristics of total EDC participants - parental factors (N=657)	22
Table 5. General characteristics of total EDC participants - child factors (N=657)	23
Table 6. Mean DNA methylation levels at age 2 at each CpG site by prenatal bisphenol A exposure levels (high (n=8) vs. low (n=51)) (Top 25 CpG sites sorted by p-values)	27
Table 7. Mean DNA methylation levels at age 6 at each CpG site by prenatal bisphenol A exposure levels (high (n=8) vs. low (n=51)) (Top 25 CpG sites sorted by p-values)	28
Table 8. Mean DNA methylation levels at age 2 at each CpG site by prenatal bisphenol A exposure levels (high (n=8) vs. low (n=51))(Top 5 CpG sites sorted by p-values at CpG island or promoter regions)	32
Table 9. Mean DNA methylation levels at age 6 at each CpG site by prenatal bisphenol A exposure levels (high (n=12) vs. low (n=49))(Top 5 CpG sites sorted by p-values at CpG island or promoter regions)	32
Table 10. Threshold point estimation for the non-linear model for the association between log ₂ (prenatal BPA) and DNA methylation levels at cg19196862 (<i>IGF2R</i>)	35
Table 11. Difference in methylation levels in cg19196862 (<i>IGF2R</i>) in 2-year children by high vs. low prenatal BPA exposures with different cut off values (n=59)	35
Table 12. Matching of ages at bisphenol A exposure and ages for DNA methylation in Table 13~16	36
Table 13. Mean DNA methylation levels at age 2 at each CpG site by postnatal bisphenol A exposure at age 2 (high (n=6) vs. low (n=25)) (Top 25 CpG sites sorted by p-values)	37
Table 14. Mean DNA methylation levels at age 6 at each CpG site by postnatal bisphenol A exposure at age 2 (high (n=6) vs. low (n=25)) (Top	

25 CpG sites sorted by p-values)	38
Table 15. Mean DNA methylation levels at age 6 at each CpG site by postnatal bisphenol A exposure at age 4 (high (n=6) vs. low (n=53)) (Top 25 CpG sites sorted by p-values)	39
Table 16. Mean DNA methylation levels at age 6 at each CpG site by postnatal bisphenol A exposure at age 6 (high (n=12) vs. low (n=47)) (Top 25 CpG sites sorted by p-values)	40
Table 17. Association between methylation at cg19196862 (<i>IGF2R</i>) and BMI and BMI Z-score (n=59)	42
Table 18. Mediation effect of methylation at cg19196862 (<i>IGF2R</i> body) on the association between prenatal BPA exposure and BMI Z-score.	45
Table 19. Sensitivity analysis for the association between methylation at cg19196862 (<i>IGF2R</i>) in 2-year children and increase in BMI and BMI Z-score (n=59)	48
Table 20. Sensitivity analysis: Association between methylation level (high 50 percentile vs. low 50 percentile) at cg19196862 (<i>IGF2R</i>) and BMI and BMI Z-score adjusting for propensity scores (n=59)	50
Supplementary Table 1. List of 594 CpG sites	82
Supplementary Table 2. Association between methylation at cg19196862 (<i>IGF2R</i>) and BMI and BMI Z-score showing R ² (n=59)	83
Supplementary Table 3. 23 Association between methylation level (upper 50 percentile vs. lower 50 percentile) at cg19196862 (<i>IGF2R</i>) and BMI and BMI Z-score adjusted for propensity scores showing R ² (n=59)	84

List of Figures

Figure 1. Flow diagram of identification of relevant studies	8
Figure 2. Process of selecting CpG sites	12
Figure 3. Causal mediation analysis	16
Figure 4. Maternal urinary BPA at second trimester in the total cohort vs. sub-cohort with methylation data	24
Figure 5. Child's urinary BPA at ages 2, 4, 6, and 8 years in total cohort vs. sub-cohort with methylation data	25
Figure 6. Left: Distribution of methylation levels at cg19196862 (<i>IGF2R</i>), Right: Violin plot showing the distribution of methylation levels at age 2 and 6 years at cg19196862 (<i>IGF2R</i>)	29
Figure 7. Methylation levels at cg19196862 (<i>IGF2R</i>) by prenatal BPA exposure at age 2 and 6 years	30
Figure 8. Generalized additive model for the association between log ₂ (prenatal BPA) and DNA methylation levels at cg19196862 (<i>IGF2R</i>) adjusted for mother's age, BMI, education, and cell type fractions	35
Figure 9. Increase in BMI and BMI Z-score and 95% confidence interval by 1 standard deviation increase of methylation levels at cg19196862 (<i>IGF2R</i>)	43
Figure 10. Mediation effect of methylation at cg19196862 (<i>IGF2R</i>) on the association between prenatal BPA exposure and BMI Z-score in boys and girls overall.	46
Figure 11. Sensitivity analysis for the increase in BMI and BMI Z-score and 95% confidence interval by 1 standard deviation increase of methylation levels at cg19196862 (<i>IGF2R</i>)	49
Supplementary Figure 1. 12 Batch effects by positions on the EPIC chips before (left) and after (right) correction (methylation data at age 2, within the selected 495 CpG sites)	85
Supplementary Figure 2. 13 Batch effects by positions on the 450K chips before (left) and after (right) correction (methylation at age 6, within the selected 495 CpG sites)	85

Introduction

Bisphenol A (BPA) is one of the world's most produced chemicals and has been used in manufacturing polycarbonate plastics, resins, thermal product receipts, food cans, dental fillings, and medical devices (Braun, 2017). BPA is widely detected in polycarbonate water bottles, food storage containers, and water supply lines. It is mainly exposed to humans by ingestion, inhalation of dust, or through skin contact (von Goetz et al. 2010). BPA is widely detected in human urine samples (Myridakis et al. 2015; Romano et al. 2015; Vandenberg et al. 2010), placenta (Balakrishnan et al. 2010), amniotic fluid and human breast milk (Vandenberg et al. 2007) suggesting intrauterine BPA exposure and continued postnatal exposure in childhood.

BPA has been indicated as an obesogen in pediatric epidemiological studies, but the results are not consistent regarding sex and ages. For boys, Vafeiadi et al. (2016) found a positive association between maternal BPA exposure and body mass index (BMI) Z-scores only in 4-year-old boys. Heopner et al. (2016) and Harley et al. (2013) reported that BPA had null effect on BMI or waist circumference (WC) in boys. For girls, Heopner et al. (2016) showed a positive relationship between maternal BPA exposure and fat mass index and WC in 7-year-old girls, whereas Vafeiadi et al. (2016) and Harley et al. (2013) found that maternal BPA exposure had negative effects on BMI Z-scores and percent body fat at 9 years old.

Animal experiments have shown the effects of maternal BPA exposure on DNA methylation and obesity in offspring in a sex-specific manner. DNA methylation patterns (high or low methylation) of offspring born to mothers exposed to BPA showed changes in DNA methylation at *Fggy* gene promoter region, and resulted in increased *Fggy* mRNA expression and weight gain only in male mice (Taylor et al. 2018). *In utero* exposure to BPA resulted in sex-specific changes in metabolic phenotypes in

mice; for example, the male mice showed a dose-dependent increase in body weight and liver weight, while female mice showed a dose-dependent decrease in body, liver, fat pad weight, and fat cell sizes (van Esterik et al. 2014). Since the association between maternal BPA exposure and obesity-related phenotypic changes was more prominent in female mice, the researchers further studied the methylation patterns in female mice. As a result, DNA methylation exhibited different patterns in the liver tissues of female offspring only (van Esterik et al. 2015).

In a children's cohort study, the second highest tertile of maternal urine BPA in second trimester of pregnancy is associated with higher *IGF2* methylation in 14-year-old children compared to the lowest tertile (Goodrich et al. 2016). Other epigenetic epidemiologic studies show that *in utero* exposure to BPA is associated with hypomethylation in *MEST* gene promoter and increased expression of *MEST* in cord blood, which is associated with an increase in the child's BMI Z-score in a sex-dependent manner (Junge et al. 2018). Changes in obesity-related methylation have been reported in epigenome-wide association studies (EWAS) in children (Huang et al. 2015; Rzehak et al. 2017; Sharp et al. 2017). However, it remains unknown whether such changes in methylation are related to prenatal environmental exposures.

The aim of this study is to determine whether DNA methylation differs according to maternal BPA exposure levels, and whether such differences in methylation leads to sex-specific BMI changes in early childhood using data from a prospective mother-child cohort study.

Methods

Study Participants

The data from the Children's Environment and Development (EDC) study was used, an ongoing prospective cohort study designed to assess the impact of early environmental exposure on physical and neurobehavioral development in children as previously described (Kim et al, 2018). Briefly, a total of 726 mother-child pairs were enrolled between 2012 and 2015 from the mothers who previously participated in the Congenital Abnormality Study. Children first visited at age 2 (n = 425) and age 4 (n = 301) and were followed up at 2-year intervals. The study included 59 children who visited at the ages of 2, 4, 6 and 8, repeatedly and whose blood DNA methylation was evaluated at ages 2 and 6. Informed consent was obtained according to the Institutional Review Board of Seoul National University School of Medicine (IRB No. 1201-010-392).

Data collection

The child's weight and height were measured by trained research staff. The height was measured on a Harpenden stadiometer (Holtain Ltd., Crymych, Wales, UK) and the weight was measured on a digital scale (150 A: Cas Co. Ltd., Seoul, Korea). BMI was calculated as $\text{weight}/\text{height}^2$ (kg/m^2). The Z-scores for height, weight and BMI were assigned according to the 2007 national growth chart of Korea (Moon et al. 2008). The questionnaires including birth history, family history, past medical history, socioeconomic status, lifestyle factors including diet and physical activity, and environmental exposure were completed by parents at each visit.

Urine BPA was measured as introduced in a previous study (Lim et al. 2017). The first morning urine was collected in conical tubes (SPL Lifesciences, Pocheon, Gyunggii-do, Korea) after an 8-hour fasting in the mother and child. Maternal urine was collected during the midterm of pregnancy (14-27 weeks, average 20 weeks of gestation). The sample was stored at -20°C in the sample laboratory (Seegene Medical Foundation, Seoul, Korea). Total BPA concentration, including free and conjugated species, was measured, and conjugated BPA species were hydrolyzed from β -glucuronidase/sulfatase. BPA concentration was quantified by high performance liquid chromatography-tandem mass spectrometry (Agilent 6410 Triple Quad LCMS; Agilent, Santa Clara, CA, USA) (Yang et al. 2003). Standard BPA solutions were analyzed with preparation blanks at 50, 25, 12.5, 6.25, 3.125 and 1.5625 μ g/L to determine standard calibration curves ($r^2 > 0.999$). If the measured concentration of the sample exceeded the maximum level of the standard BPA solution, the sample was diluted (1:1) and analyzed again. Samples were analyzed again if the detected concentration was not within 20% of the standard calibration curve. The detection limit (LOD) ranged from 0.031 to 0.212 μ g/L depending on batches, and an LOD value of $0.212/\sqrt{2}$ was used. Throughout the entire analysis, creatinine-adjusted BPA values were used in the unit of μ g/g creatinine (Calafat et al. 2005). Since the distribution of creatinine-adjusted BPA was skewed to the right, the \log_2 transformed BPA was used for normalization.

DNA methylation assessment

DNA methylation was measured in blood samples obtained at ages 2 and 6. The quality of the DNA sample was confirmed by a

NanoDrop®ND-1000UV-Vis spectrophotometer. Samples containing whole genomic DNA were selected after electrophoresis on an agarose gel and diluted to 50 ng/μL according to the quantification of Quanti-iT Picogreen (Invitrogen). At least 500ng of gDNA was converted to weight sulfate according to the Zymo EZ DNA methylation kit. Bisulfite transformed DNA was amplified for use in a single BeadChip (x1000). The Illumina Infinium HumanMethylation 450K BeadChip was used to obtain the 450,000 CpG locus sequence used in blood samples for 6 years of age (Illumina, San Diego, CA, USA). Since the HumanMethylation 450K BeadChip became unavailable at Illumina, Infinium HumanMethylation EPIC BeadChip was used to generate 850,000 CpG locus sequence from blood sample at 2 years of age (Illumina, San Diego, CA, USA). The amplified DNA was fragmented and hybridized by a 50mer capture probe at the CpG locus. In the allele-specific single nucleotide extension assay, primers were extended with a polymerase and labeled nucleotide mix (Two-Color Extension Master Mix), stained with staining and anti-staining reagents, then washed and coated. The image was read by Illumina BeadArray reader and the image intensity was extracted by Illumina's GenomeStudio software. Microarrays were processed at Macrogen (Seoul, Korea).

Raw data was extracted as the beta value of each CpG. The beta value was calculated by taking the ratio of the methylated signal intensity to the total of the methylated and unmethylated signals of the 5th carbon (% 5mC) ranging from 0 (no methylation) to 100 (fully methylated). Each signal was subtracted from the control as a background signal. Gene enrichment and functional annotation analysis of each probe list was performed using Database for Annotation, Visualization, and integrated Discovery (<http://david.abcc.ncifcrf.gov/home.jsp>).

Quality control for methylation data

The detection p-value <0.05 was applied as filtering criteria. Array CpG probes with a detection p-value of 0.05 or higher in samples of 25% or more were excluded from the filter because of the high probability of a high signal-to-noise ratio. The filtered data were standardized by the Beta Mixture Quantile (BMIQ) method (Teschendorff et al. 2013). For the HumanMethylation EPIC BeadChip (850K), 865,688 CpG sites were analyzed from a total of 866,297 CpG sites after excluding CpG sites with not available (NA) values for BMIQ normalization in at least one sample. For the HumanMethylation 450K BeadChip, CpG sites with NA values of at least one sample for BMIQ normalization were excluded. At the 485,577 CpG sites of the raw data, 460,960 CpG sites remained for analysis. In addition, non-CpG loci and CpG sites corresponding to X or Y chromosomes were excluded from further analysis. The removal of SNP-related CpG sites is described in the next step for CpG sites targeting. Samples from 59 study participants at ages 2 and 6 were analyzed in a single batch. The placement effect by chip and location was adjusted using R ComBat package (Johnson et al. 2007). We used unadjusted data since there was only one batch at each age, and the batch effects by positions were not significant (Supplementary Figure 1 and 2).

Systematic review of literature

Since the question of interest was whether DNA methylation plays a mediating role in the effects of maternal BPA exposure on childhood adiposity, candidate gene analysis was performed rather than EWAS. EWAS are widely performed for detecting phenotype-associated differentially

methyated positions (DMPs) or regions (DMRs) over the entire epigenome. However, in this study, hypothesis was established such as “epigenetic mechanisms are involved in the association between prenatal BPA exposure and child’s BMI.” Thus, CpG sites were targeted to those that are already known to be associated with obesity or adiposity.

To target specific CpG sites that are known to be associated with obesity or adiposity, systematic review was performed to select previous EWAS. Pubmed and EMBASE were searched on February 7, 2019, using keywords such as ““Epigenome-wide association study” and (Obesity or “body mass index” or BMI or adiposity or adipose or fat or “waist circumference” or “fat mass index”)”. The selection criterion was EWAS conducted in relation with obesity or adiposity in healthy adult or children. EWAS conducted in patients with specific diagnoses such as leukemia or prostate cancer were excluded. To increase specificity, EWAS performed in relation with clinical traits that are related with obesity were not included such as insulin resistance, metabolic syndrome, diabetes, or dyslipidemia. In other words, the only studies that investigated the indices that represent adiposity or obesity were specifically included.

A total of 91 and 133 articles were found in Pubmed and EMBASE, respectively. After excluding 79 duplicated articles, a total of 148 articles were left for the review of abstracts (Figure 1). Among 148 articles, 121 articles were irrelevant, and 12 were additionally excluded due to insufficient information or irrelevance. Three articles were added after manual bibliographic search, ultimately leaving 15 articles for the selection of relevant CpG sites (Al Muftah et al. 2016; Aslibekyan et al. 2015; Campanella et al. 2018; Demerath et al. 2015; Dhana et al. 2018; Huang et al. 2015; Kvaloy et al. 2018; Lin et al. 2017; Rzehak et al. 2017; Sayols-Baixeras et al. 2017; Sharp et al. 2015; Sharp et al. 2017; Wahl et

al. 2017; Wilson et al. 2017; Xu et al. 2018) (Table 1).

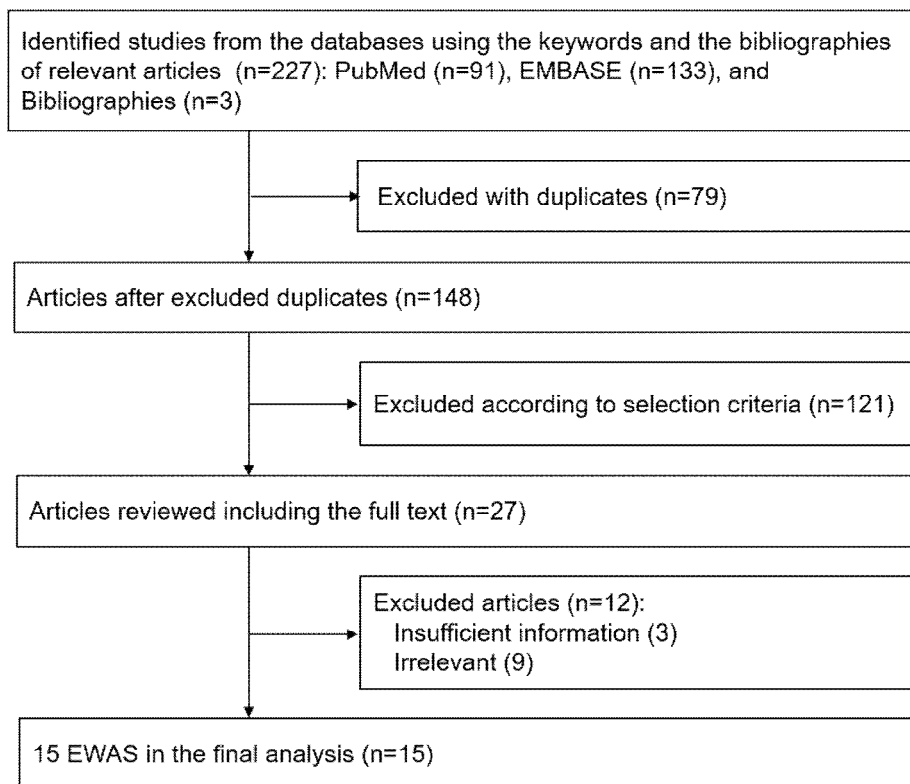


Figure 1. Flow diagram of identification of relevant studies

Abbreviation: EWAS, epigenome-wide association studies

Table 1. Previous epigenome-wide association studies for the association between methylation and obesity

Study	Study population	Cohort (or case/control study)	Age for methylation data (years)	Number of study participants	Adiposity measures	Tissue of methylation data	No. of associated cg sites	Cell type fraction adjusted	Reference tables
Aslibekyan et al. 2015	US adults	GOLDN	Mean 49	991 (Male 476/Female 515)	BMI, WC	CD4+ T-cells in blood	13	Not applicable	Table 2,3
Demerath et al. 2015	African American adults	ARIC, GOLDN study	Average 56	2,097 (Male 755/Female 1342)	BMI, WC	Blood leukocytes	45	Adjusted	Table 2,3
Huang et al. 2015	UK children seeking treatment for obesity at the tertiary pediatric hospital		Median 12.6	108 (54 cases/54 controls)	Obese vs. lean group	Whole blood	129	Compared between case and control but not adjusted	Table 2
Sharp et al. 2015	UK newborns	ALSPAC	0	1,018 mother-offspring pairs	Maternal obese vs. normal weight	Cord blood	110	Adjusted	Supp Table 2
Al Muftah et al. 2016	Arab and UK adults	Qatari family study (discovery), TwinsUK cohort (validation)	Mean 36.3 for men, 39 for women	123 (discovery), 877 (validation)	BMI	Whole blood	39	Adjusted	Table 2
Lin et al. 2017	Singapore neonates	GUSTO	0	987 mother-offspring pairs	Birthweight	Cord blood	8	Adjusted	Table 3
Rzehak et al. 2017	Germany, Belgium, Italy, and Spain preschool children	CHOP	5.5	374	BMI, FMI, FFMI	Whole blood	256	Adjusted	Supp Table 2

Sayols-Baixas et al. 2017	Spanish and US adults	REGICOR (discovery), Framingham Offspring Study (validation)	35-79	648 (discovery), 2,568 (validation)	BMI, WC	Whole blood	103	Not mentioned	Table 2,3
Sharp et al. 2017	European and hispanic newborns and adolescents	meta-analysis of 19 cohorts (PACE consortium)	0-18	9,340 mother-offspring paris	Maternal pre-pregnancy BMI	Child's whole blood or cord blood	86	Mixed (meta-analysis)	Table 3
Wahl et al. 2017	European and Indian-Asian adults	EPICOR, KORA, LOLIPOP	Mean 51.0-61.0	5,347 (514 EPICOR, 293 KORA, 2,680 LOLIPOP)	BMI	Whole blood	187	Adjusted	Supp Table 3
Wilson et al. 2017	US white, non-Hispanic women	The Sister Study	35-74	871 (discovery), 187 (validation)	BMI	Whole blood	15	Adjusted	Table 3
Campanella et al. 2018	Italy, Netherlands, and Norwegian adults	EPIC-Netherlands, NOWAC, EnviroGenoMarkers, EPIC-Italy	Not specified (adults)	1,941 (discovery), 358 (validation)	BMI, WC, WHR, WHtR	Blood leukocytes	59	Adjusted	Table 1
Dhana et al. 2018	Netherlands adults	Rotterdam Study, ARIC study	45-64	1,450 (discovery), 2,097 (validation)	BMI, WC	Blood leukocytes	20	Adjusted	Table 2,3
Kvaloy et al. 2018	Norwegian women	HUNT study	23-31	120 (60 cases/60 controls)	Obese vs. lean group	Whole blood	10	Adjusted	Table 2
Xu et al. 2018	US adults		18-50	510	BMI	Whole blood	20	Adjusted	Table 2

(Abbreviation; BMI, body mass index; WC, waist circumference; WHR, waist hip ratio)

Selection of candidate CpG sites

CpG sites for obesity-related parameters such as BMI, BMI Z-score, waist circumference, and fat mass index were extracted from the selected EWAS that examined the association between epigenome-wide DNA methylation and obesity in adults and children, which were added up to 1,100 CpG sites. Redundant CpG sites (210 CpG sites) reported in more than two studies were excluded, leaving 900 CpG sites (Figure 2). Among these, 135 CpG sites were located in the single base extension of the existing single nucleotide polymorphism (SNP), 49 CpG sites showed a minor allele frequency (MAF) ≥ 0.05 in the SNP of the target region, and 25 CpG sites corresponded to the both criteria, adding up to 209 CpG sites. These CpG sites were excluded from the analysis as they could be confused by the effects of SNPs, thus leaving 681 CpG sites.

To compare DNA methylation status at ages 2 and 6, 430,101 overlapping CpG sites were selected from CpG sites at ages 2 (HumanMethylation EPIC BeadChip, 865,688 CpG sites) and 6 (HumanMethylation 450K BeadChip, 460,960 CpG sites). Finally, the overlapping 594 CpG sites were selected from 681 CpG sites from systematic review of literature and 430,101 CpG sites from the EDC data. The list of 594 CpG sites is shown in Supplementary Table 1.

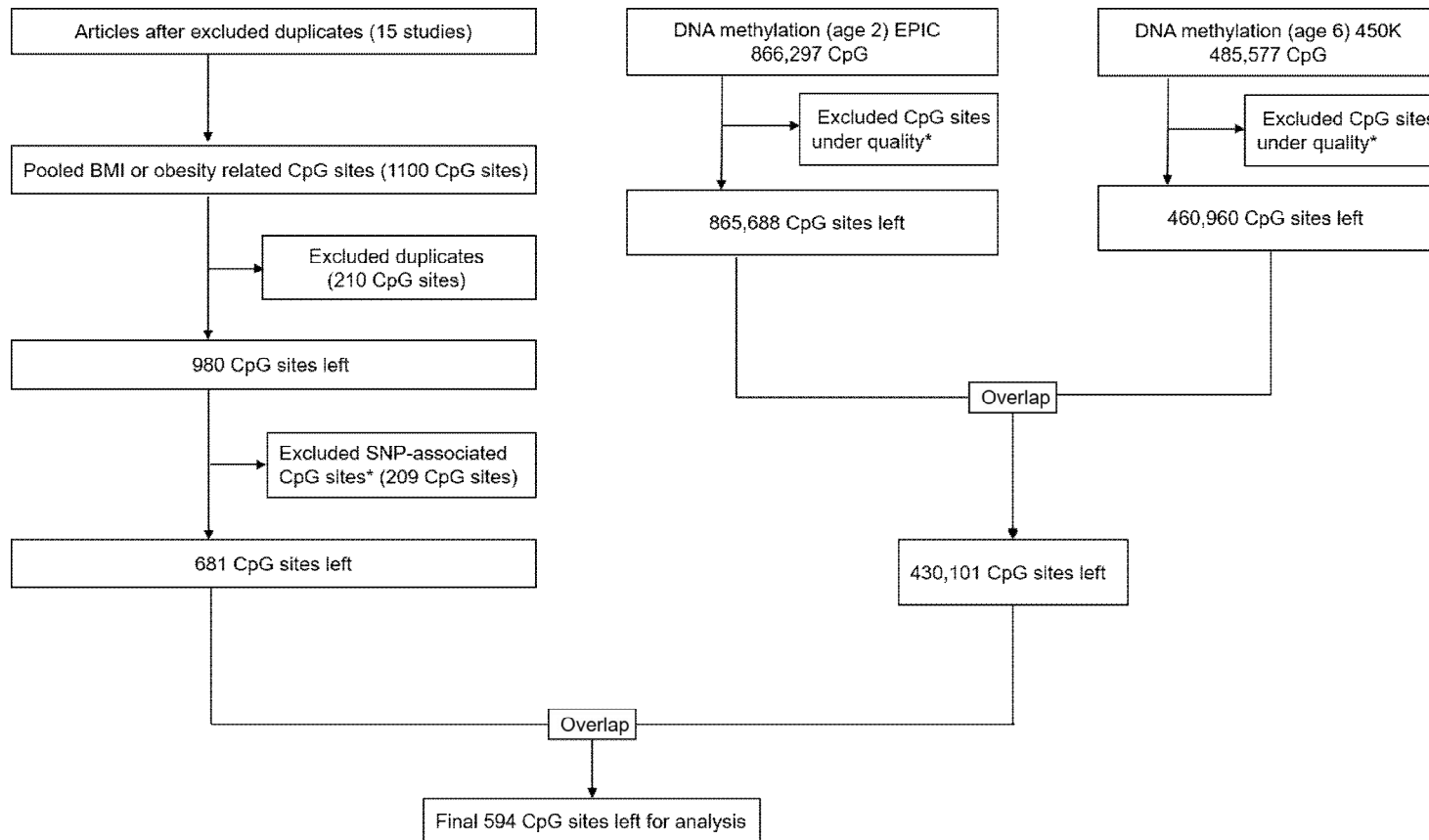


Figure 2. Process of selecting CpG sites

Covariates

To investigate the association between DNA methylation levels and BMI or BMI Z-scores at 2, 4, 6, and 8 years of age, the model included the following covariates: mother's age during pregnancy (years), mother's and father's BMI when the child was 2 years old (kg/m^2) (pre-pregnant BMI was unavailable), mother's education level (junior high school graduates, high school graduates, college graduates, or attending graduate school), premature birth (<37 or ≥ 37 weeks), low birth weight (<2500 or $\geq 2500\text{g}$), duration of breastfeeding (<6 or ≥ 6 months), caloric intake (kcal/day) in children aged 4, 6 and 8 (several missing values at age 2), and urine BPA (in $\mu\text{g}/\text{g}$ creatinine) in children aged 4, 6, and 8 years old (several missing values at age 2), which were adjusted at the corresponding ages. The child's urine BPA level was measured in the same method as in mothers. Maternal information obtained by questionnaires was confirmed by a trained research staff during face-to-face interview. Diet information was obtained from a food intake frequency questionnaire (FFQ) by a nutritionist. The proportions of cell types such as CD8⁺ T cells, CD4⁺ T cells, natural killer (NK) cells, B cells, monocyte, and neutrophils were adjusted.

For the sensitivity analysis, the following covariates were additionally adjusted: multiple births (singleton or twin/triplet), mother's smoking (smoking during pregnancy, smoked before pregnancy, and never smoked), and mother's alcohol consumption (drank during pregnancy, drank before pregnancy, and never drank).

Statistical analysis

To evaluate the general characteristics of the study participants (N = 59), we used Student's t-test for continuous variables and the Fisher's exact test for categorical variables. Student's t-test and chi-square test were applied to compare the general characteristics of participants between the entire EDC cohort participants and a subset of the EDC cohort where DNA methylation data were available. The characteristics of the study participants were analyzed using Student's t-test for the continuous variable, and chi-square test or Fisher's exact test for categorical variables to compare two groups.

CpG sites of which the methylation level differed depending on prenatal BPA levels were sought at ages 2 and 6. Prenatal BPA exposure groups were classified as low ($<2.68 \mu\text{g/g}$ creatinine) vs. high ($\geq 2.68 \mu\text{g/g}$ creatinine) according to the 80th percentile of maternal BPA levels in the second trimester of pregnancy in mothers from the entire EDC cohort. Sensitivity analysis was performed by using 75th percentile and 90th percentile.

The distribution of methylation at individual CpG site was inspected. Among 594 CpG sites, 565 CpG sites showed unimodal distribution while the other 29 sites showed bimodal (two peaks) or trimodal (three peaks) distributions. For unimodal CpG sites, Student's t-test was used to evaluate the differences in the mean levels of DNA methylation by prenatal BPA exposure groups. Bimodal or trimodal CpG sites were excluded from further analysis. Student's t-test was used again to test the differences in the mean levels of DNA methylation by prenatal BPA exposure groups within promoter regions (5' UTR, 3' UTR, TSS200, TSS1500) and CpG islands only. The differences in the mean level of DNA methylation at 565 CpG sites at age 2, 6, 6, and 6 years by postnatal BPA

exposure at ages 2, 2, 4, and 6 years, respectively, by using t-test. For multiple comparisons, the significance level was defined as false detection rate (FDR) corrected p-value <0.05 by the Benjamini and Hochberg method (Benjamini and Hochberg 1995).

Generalized additive model was used to inspect non-linearity in the association between prenatal BPA levels and methylation levels at cg19196862 (*IGF2R*), adjusting for mother's age, BMI, and education levels. Threshold point was determined by using `thresht` function from R HEAT package.

Linear regression analysis was conducted to investigate the association between the level of methylation at the CpG site and BMI or BMI Z-scores at ages 2, 4, 6, and 8, adjusting for the covariates introduced earlier. The cell type fractions in blood samples were estimated by using the adult leukocyte reference panel by the method proposed by Houseman et al. (2012). The `Minfi` R package was used to estimate the cell type fraction of each blood sample (Aryee et al. 2014). The estimates from linear regression were multiplied by the standard deviation (SD) of each CpG site to produce a change in BMI or BMI Z-score with 1 SD change in methylation level. We analyzed sex-specific effects of DNA methylation on obesity in children by introducing an sex interaction term into the regression analysis. To evaluate the statistical significance of the regression analysis, a p-value <0.05 was used.

For sensitivity analysis, firstly, for the linear regression analysis for DNA methylation and BMI or BMI Z-score, multiple birth (singleton or multiple), smoking, and drinking were additionally adjusted for the main model. Secondly, a propensity score was calculated for methylation levels at cg19196862 as a binary variable (upper 50 percentile vs. lower 50

percentile) by using the following covariates: mother's age at pregnancy, mother's and father's BMI, mother's education level, child's sex, preterm birth or not (<37 weeks), underweight at birth or not (<2500g), breastfeeding for ≥ 6 months or not, and cell type fraction. Then the propensity score was solely adjusted for the the linear regression analysis for DNA methylation and BMI or BMI Z-score.

Causal mediation analysis was performed to estimate the mediating effects of DNA methylation from prenatal BPA exposure to child's BMI or BMI Z-score. Causal mediation analysis is a method to dissect the total effect into direct and indirect effect. The indirect effect is transmitted through a mediator (Zhang et al, 2016).

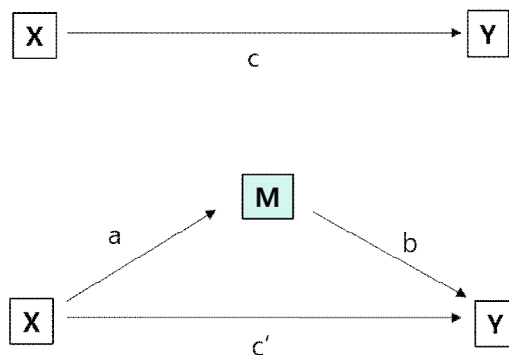


Figure 3. Causal mediation analysis

$$Y = i_1 + cX + e_1 \quad [1]$$

$$Y = i_2 + c'X + bM + e_2 \quad [2]$$

$$M = i_3 + aX + e_3 \quad [3]$$

where X, Y, and M denotes explanatory variable, outcome variable, and mediator, respectively (Zhang et al, 2016) (Figure 3). c is a coefficient for the association between X and Y, and association is defined as a total causal effect. c' is the coefficient for the effect of X on Y while adjusting

for M. b is the effect of M on Y. e_1 , e_2 , and e_3 are residuals and i_1 , i_2 , and i_3 are intercepts.

From the equations above, M from [3] can be substituted to M in [2], resulting in the equation below.

$$\begin{aligned} Y &= i_2 + c'X + b(i_3 + aX + e_3) + e_2 \\ &= i_2 + (c' + ab)X + bi_3 + be_3 + e_2 \end{aligned} \quad [4]$$

where c' is defined as direct effect and ab is defined as indirect effect (mediation effect), which are added up to the total effect, c . R mediation package provides the estimation of these effects, and performs sensitivity analysis to examine the robustness of the analysis, thereby computing average direct effect (ADE) and average indirect effects. Average indirect effect is a subtraction of direct effect from the total effect, and defined as average causal mediating effect (ACME).

In this study, X denotes prenatal BPA exposure, Y denotes child's BMI or BMI Z-score, and M represents DNA methylation. Coefficients c' and ab were assessed by linear regression analysis adjusted by the same covariates as in the main analysis. Using the R mediation package, we applied nonparametric bootstrap by 1,000 simulations and estimated ACME and ADE. The mediated rate represents the average size of the mediated total effect (ACME + ADE). For statistical analysis, SAS (v9.4) (Cary, NC, USA) and R software (v3.2.1) (R Development Core Team <https://cran.r-project.org/>) were used.

Results

General characteristics of participants

Table 2 and 3 shows the comparison of general characteristics of participants between the two groups by prenatal BPA exposure (high vs. low). There was no significant differences in parental factors (mother's age at pregnancy, and mother's and father's BMI before pregnancy), child factors (gender, multiple births, preterm birth, underweight, breastfeeding duration, postnatal BPA exposure, total caloric intake, BMI, BMI Z-score), and overall cell type fraction between the two groups (excluding the fraction of B cells). The mean prenatal urine BPA levels in the low vs. high BPA exposure groups were $1.34 \pm 0.60\mu\text{g/g}$ creatinine (up to $2.77\mu\text{g/g}$ creatinine) and $7.92 \pm 4.97\mu\text{g/g}$ creatinine (up to $18.38\mu\text{g/g}$ creatinine), respectively.

Table 4 and 5 shows the clinical characteristics of all participants in the EDC cohort without missing clinical data ($N = 657$) and a comparison of clinical characteristics between 59 children with methylation data analyzed in this sub-study and the remaining 598 children without methylation data. Compared to the entire cohort ($n=598$), the children included in this sub-study had a greater mother's BMI, greater percentages of mother's current smoking and drinking, greater child's BMI and BMI Z-score at ages 4, 6, and 8, total caloric intake at age 2, and lower levels of postnatal BPA exposure at ages 4 and 8. Other maternal factors (prenatal BPA exposure, mother's age at pregnancy, mother's level of education) and child factors (gender, twin births, preterm birth, underweight, and duration of breastfeeding) did not differ between the two groups (Table 5).

Maternal urinary BPA level during the second trimester was $2.02 \pm 2.52\mu\text{g/g}$ creatinine in the total cohort, and $2.23 \pm 2.91\mu\text{g/g}$ creatinine in the

sub-study with the methylation data (Table 2 and Table 4). Child's urinary BPA was ranged from 3.34 to 6.32 $\mu\text{g/g}$ creatinine in the total cohort while it was ranged from 1.9 to 3.52 $\mu\text{g/g}$ creatinine in the sub-study during the ages of 4 to 8 (Table 3 and Table 5). According to the National Environmental Health Survey (Korea Ministry of Environment, 2019), geometric mean urinary BPA was 1.48 $\mu\text{g/g}$ creatinine (95% confidence interval (CI); 1.40, 1.57) in adults in 2014, and 2.83 $\mu\text{g/g}$ creatinine (95% CI; 2.41, 3.33) in preschool children in 2017. Distribution of prenatal (Figure 4) and postnatal BPA (Figure 5) are shown in the entire cohort and the sub-study with the methylation data available.

Table 2. General characteristics of the sub-cohort according to prenatal BPA exposure level – parental factors (n=59).

Participants	Variables	Low maternal BPA (n=51)	High maternal BPA (n=8)	p-value	
Mother	Age at pregnancy (years)	31.3 ± 3.8	29.5 ± 3.4	0.209	
	Pre-pregnancy BMI (kg/m ²)	22.7 ± 3.4	24.0 ± 6.6	0.594	
	Educational level	Middle school graduate	0 (0%)	0 (0%)	NA
		High school graduate	7 (13.7%)	2 (25.0%)	
		College graduate	39 (76.5%)	3 (37.5%)	
		Graduate school	5 (9.8%)	3 (37.5%)	
	Urinary bisphenol A at second trimester (µg/g creatinine)	Urinary BPA	1.34 ± 0.60	7.92 ± 4.97	0.007
		Maximum urinary BPA	2.77	18.38	
	Smoking during pregnancy	Never smoker	27 (52.9%)	2 (25.0%)	NA
		Smoke tobacco before pregnancy	19 (37.3%)	5 (62.5%)	
		Smoked tobacco during pregnancy	5 (9.8%)	1 (12.5%)	
	Alcohol consumption during pregnancy	Never drinker	11 (26.2%)	0 (0%)	NA
		Consume alcohol before pregnancy	20 (47.6%)	3 (50%)	
Consumed alcohol during pregnancy		11 (26.2%)	3 (50%)		
Father	Pre-pregnancy BMI (kg/m ²)	25.5 ± 3.4	25.0 ± 3.3	0.692	

Table 3. General characteristics of the sub-cohort according to prenatal BPA exposure level – child factors (n=59).

Variables		Low maternal BPA (n=51)	High maternal BPA (n=8)	p-value
Sex	Male	23 (45.1%)	5 (62.5%)	0.359
	Female	28 (54.9%)	3 (37.5%)	
Multiple birth	Singleton	46 (90.2%)	6 (75%)	0.238
	Multiple	5 (9.8%)	2 (25%)	
Preterm (<37 weeks)	No	46 (90.2%)	5 (62.5%)	0.059
	Yes	5 (9.8%)	3 (37.5%)	
Underweight at birth (<2500g)	No	46 (90.2%)	8 (100%)	0.469
	Yes	5 (9.8%)	0 (0%)	
Breastfeeding for \geq 6 months	Yes	26 (51.0%)	4 (50%)	1.000
	No	25 (49.0%)	4 (50%)	
BPA exposure level (μ g/g creatinine)	4 years	3.49 \pm 2.53	3.68 \pm 2.07	0.841
	6 years	3.82 \pm 3.26	4.13 \pm 2.63	0.799
	8 years	2.05 \pm 1.73	0.98 \pm 1.36	0.101
Total calorie intake (kcal/day)	4 years	1464.3 \pm 333.5	1664.2 \pm 481.5	0.144
	6 years	1574.5 \pm 372.9	1633.1 \pm 533.7	0.699
	8 years	1583.5 \pm 397.9	1568.9 \pm 493.7	0.926
BMI (kg/cm ²)	2 years	16.6 \pm 1.2	16.5 \pm 1.2	0.782
	4 years	16.0 \pm 1.2	15.7 \pm 0.7	0.502
	6 years	16.4 \pm 1.8	16.3 \pm 1.3	0.925
	8 years	17.7 \pm 2.7	17.4 \pm 1.8	0.745
BMI Z-score	2 years	-0.06 \pm 0.79	-0.18 \pm 0.76	0.699
	4 years	0.23 \pm 0.88	0.06 \pm 0.62	0.588
	6 years	0.31 \pm 0.95	0.29 \pm 0.84	0.972
	8 years	0.40 \pm 1.08	0.31 \pm 0.82	0.822
Cell type fraction	CD4 T cell	0.20 \pm 0.04	0.21 \pm 0.04	0.613
	CD8 T cell	0.15 \pm 0.05	0.18 \pm 0.03	0.165
	NK cell	0.04 \pm 0.04	0.05 \pm 0.05	0.606
	B cell	0.19 \pm 0.04	0.15 \pm 0.04	0.020
	Monocyte	0.05 \pm 0.02	0.04 \pm 0.02	0.505
	Neutrophil	0.35 \pm 0.09	0.36 \pm 0.08	0.796

Table 4. General characteristics of total EDC participants – parental factors (N=657)

Participants	Variables	DNA methylation data unavailable (N=598)	DNA methylation data available (N=59)	p-value	
Mother	Age at pregnancy (years)	31.64 ± 3.57	31.07 ± 3.77	0.263	
	Pre-pregnancy BMI (kg/m ²)	21.75 ± 2.81	22.86 ± 3.92	0.042	
	Educational level	Middle school graduate	0	0	0.730
		High school graduate	58 (17.9%)	9 (15.3%)	
		College graduate	232 (71.6%)	42 (71.2%)	
		Graduate school	34 (10.5%)	8 (13.6%)	
	Urinary bisphenol A at second trimester (ug/g creatinine)	Urinary BPA	2.02 ± 2.52	2.23 ± 2.91	0.570
		Maximum urinary BPA	31.08	18.38	
	Smoking during pregnancy	Never smoker	256 (82.6%)	29 (49.2%)	<0.0001
		Smoke tobacco before pregnancy	50 (16.1%)	24 (40.7%)	
		Smoked tobacco during pregnancy	4 (1.3%)	6 (10.2%)	
	Alcohol consumption during pregnancy	Never drinker	89 (33.5%)	11 (22.9%)	<0.0001
Consume alcohol before pregnancy		157 (59.0%)	23 (47.9%)		
Consumed alcohol during pregnancy		20 (7.5%)	14 (29.2%)		
Father	Pre-pregnancy BMI (kg/m ²)	24.76 ± 2.91	25.44 ± 3.35	0.110	

Table 5. General characteristics of total EDC participants – child factors (N=657)

Participants	Variables		DNA methylation data unavailable (N=598)	DNA methylation data available (N=59)	p-value
Child	Sex	Male	174 (53.7%)	28 (47.5%)	0.377
		Female	150 (46.3%)	31 (52.5%)	
	Multiple birth	Singleton	301 (92.9%)	52 (88.1%)	0.210
		Multiple	23 (7.1%)	7 (11.9%)	
	Preterm (<37 weeks)	No	302 (93.2%)	51 (86.4%)	0.075
		Yes	22 (6.8%)	8 (13.6%)	
	Underweight at birth (<2500g)	No	305 (94.1%)	54 (91.5%)	0.447
		Yes	19 (5.9%)	5 (8.5%)	
	Breastfeeding for ≥6 months	Yes	220 (67.9%)	38 (64.4%)	0.599
		No	104 (32.1%)	21 (35.6%)	
	BPA exposure level (µg/g creatinine)	4 years	6.32 ± 18.84	3.52 ± 2.46	0.002
		6 years	3.7 ± 7.89	3.86 ± 3.16	0.769
		8 years	3.34 ± 4.94	1.9 ± 1.71	0.000
	Total caloric intake (kcal/day)	4 years	1424 ± 418.3	1491.4 ± 358.6	0.238
		6 years	1468.7 ± 360.9	1582.4 ± 393.3	0.025
		8 years	1491.6 ± 292.6	1581.4 ± 407.9	0.119
	BMI (kg/cm ²)	2 years	16.49 ± 1.48	16.59 ± 1.2	0.614
		4 years	15.57 ± 1.29	15.99 ± 1.13	0.017
		6 years	15.73 ± 1.81	16.37 ± 1.73	0.011
		8 years	16.75 ± 2.42	17.68 ± 2.56	0.009
	BMI Z-score	2 years	-0.16 ± 0.96	-0.08 ± 0.78	0.529
		4 years	-0.18 ± 1.08	0.21 ± 0.85	0.002
		6 years	-0.15 ± 1.05	0.3 ± 0.93	0.002
		8 years	-0.03 ± 1.08	0.39 ± 1.04	0.008

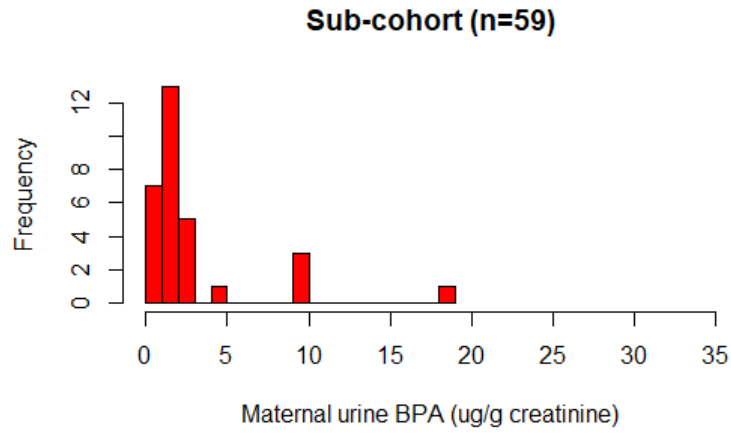
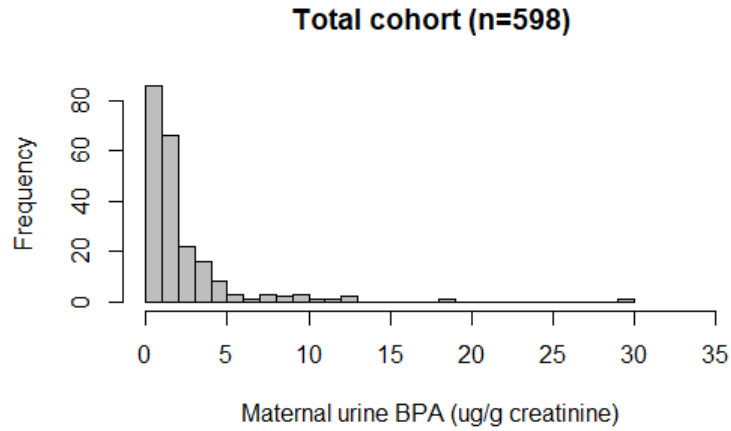
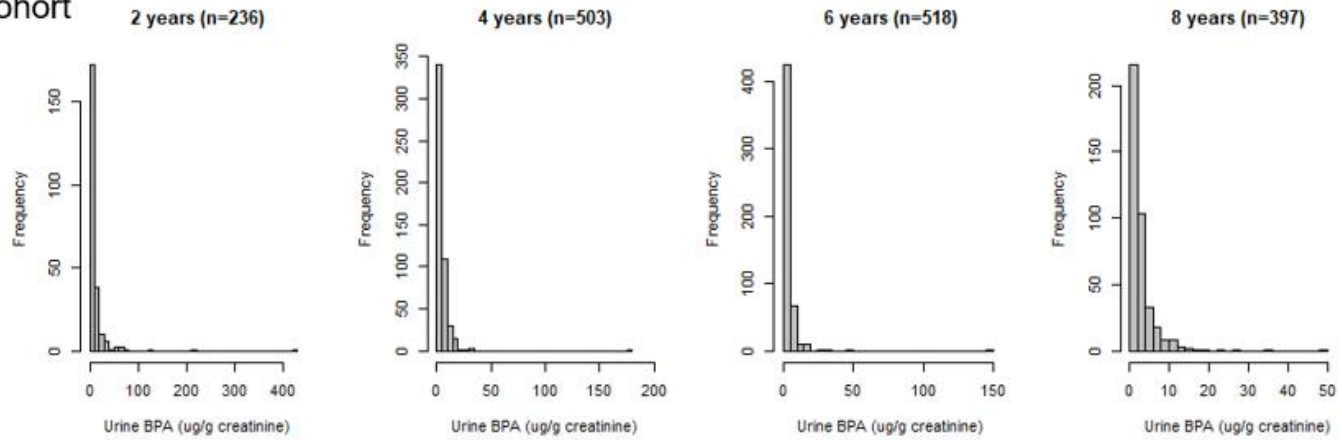


Figure 4. Maternal urinary BPA at second trimester in the total cohort vs. sub-cohort with methylation data

Total cohort



Sub-cohort

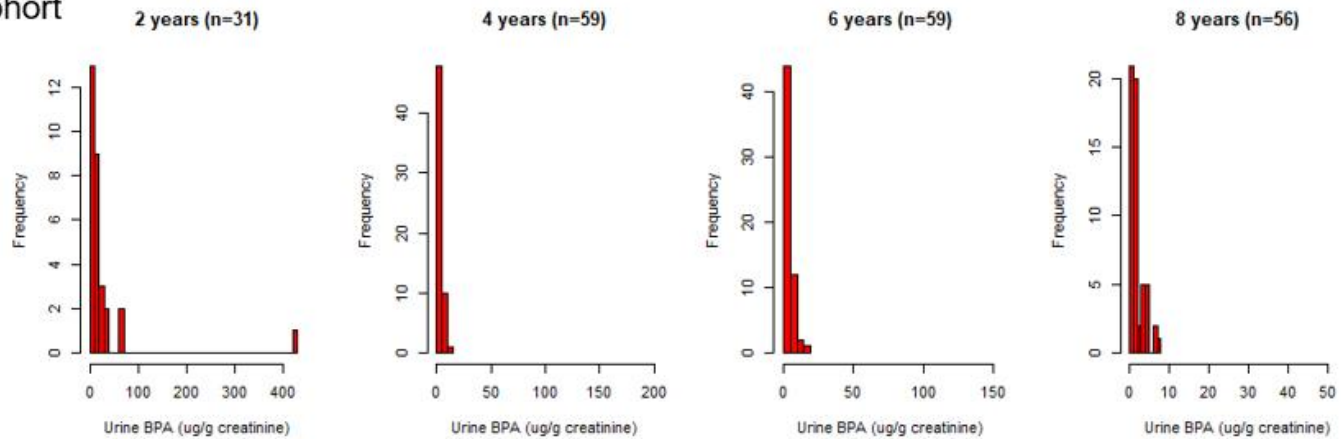


Figure 5. Child's urinary BPA at ages 2, 4, 6, and 8 years in total cohort vs. sub-cohort with methylation data

Differential methylation levels in children at ages 2 and 6 years according to prenatal BPA exposure

A total of 594 target CpG sites were compared between the prenatal high-exposure group (n = 8) and the low-exposure group (n = 51) analyzed in the blood of 2- and 6-year-old children. At age 2, cg19196862 was significantly different between the high vs. low BPA exposure group with an FDR-corrected p value <0.05 (Table 6). At 6 years of age, no CpG sites were significantly different between the two groups (Table 7).

Table 6. Mean DNA methylation levels at age 2 at each CpG site by prenatal bisphenol A exposure levels (high (n=8) vs. low (n=51)) (Top 25 CpG sites sorted by p-values)

CpG site	High prenatal BPA		Low prenatal BPA		UCSC Gene Name	UCS C Ref Gene Group	Relation to UCSC CpG Island	p_value	FDR corrected p-value
	Mean	SD	Mean	SD					
cg19196862	0.9504	0.0112	0.9593	0.00416	<i>IGF2R</i>	Body		0.000302	0.045
cg26899718	0.6132	0.0293	0.5946	0.014	<i>SMPD3</i>	Body	N_Shore	0.009515	0.942
cg15913725	0.9549	0.0106	0.9332	0.019	<i>TSSC1</i>	Body	Island	0.014242	0.993
cg20117675	0.8045	0.0308	0.821	0.0132	<i>DHX16</i>	TSS1500	S_Shore	0.016109	0.993
cg13123009	0.4087	0.0249	0.3876	0.0262	<i>LY6G6E</i>	TSS200		0.030571	0.993
cg07822775	0.8543	0.0251	0.8651	0.01	<i>PCSK6</i>	Body		0.038812	0.993
cg15357118	0.5461	0.0374	0.5166	0.0354	<i>UGGT1</i>	Body		0.041254	0.993
cg24217948	0.8647	0.0439	0.8974	0.0242	<i>SETBP1</i>	5'UTR	S_Shore	0.045405	0.993
cg26666886	0.0845	0.0117	0.0937	0.0131	<i>ANKRD11</i>	TSS1500	S_Shore	0.046472	0.993
cg27115863	0.5588	0.0212	0.5423	0.0256				0.051817	0.993
cg06690548	0.9354	0.0165	0.923	0.0167	<i>SLC7A11</i>	Body		0.053101	0.993
cg14017402	0.5045	0.0509	0.4677	0.0432				0.0583	0.993
cg00852675	0.8629	0.0265	0.8821	0.0237	<i>LOC728743</i>	Body	Island	0.058905	0.993
cg27267258	0.9439	0.0124	0.9531	0.0137	<i>ANKRD11</i>	Body		0.06044	0.993
cg10814005	0.1203	0.0243	0.1296	0.0096	<i>GPR68</i>	5'UTR		0.062934	0.993
cg01806722	0.9431	0.0103	0.9503	0.01	<i>MAML2</i>	Body		0.068761	0.993
cg09230763	0.8328	0.0461	0.8007	0.0434	<i>MAP3K6</i>	Body	Island	0.070708	0.993
cg24824917	0.0848	0.0159	0.0958	0.0145			N_Shelf	0.071163	0.993
cg10179300	0.8959	0.0231	0.9116	0.0185	<i>TRIO</i>	Body	S_Shelf	0.072717	0.993
cg02286155	0.6565	0.0214	0.671	0.0182			N_Shore	0.07424	0.993
cg13781414	0.8025	0.0354	0.8257	0.0261	<i>NACC2</i>	5'UTR		0.081159	0.993
cg15059608	0.0783	0.0117	0.0706	0.0115	<i>C3orf14</i>	TSS1500	S_Shore	0.085329	0.993
cg19358373	0.5599	0.043	0.5877	0.035			S_Shore	0.087457	0.993
cg02716826	0.4627	0.0362	0.4396	0.0271	<i>SUGT1P1; AQP3</i>	Body; Body	N_Shore	0.090301	0.993
cg18330571	0.8502	0.0289	0.8311	0.0305	<i>EBF3</i>	Body	Island	0.09059	0.993

Table 7. Mean DNA methylation levels at age 6 at each CpG site by prenatal bisphenol A exposure levels (high (n=8) vs. low (n=51)) (Top 25 CpG sites sorted by p-values)

CpG site	High prenatal BPA		Low prenatal BPA		UCSC Gene Name	UCSC Ref Gene Group	Relation to UCSC CpG Island	p_value	FDR corrected p-value
	Mean	SD	Mean	SD					
cg13139542	0.914	0.028	0.938	0.013				0.0012	0.190
cg04869770	0.797	0.033	0.824	0.016	<i>PBX1</i>	Body		0.0013	0.190
cg21186778	0.836	0.022	0.856	0.020	<i>RCLI</i>	Body		0.0200	0.956
cg03523676	0.599	0.036	0.630	0.025	<i>CPNE6</i>	TSS1500		0.0209	0.956
cg04984663	0.946	0.010	0.955	0.012				0.0228	0.956
cg14204100	0.960	0.008	0.967	0.007	<i>KIFC1</i>	Body	N_Shelf	0.0313	0.956
cg26093966	0.931	0.017	0.917	0.013			S_Shelf	0.0318	0.956
cg23827531	0.346	0.023	0.363	0.018	<i>FAM107A</i>	1stExon		0.0403	0.956
cg03862225	0.037	0.006	0.033	0.005	<i>CTBP2</i>	TSS1500	Island	0.0409	0.956
cg13084458	0.065	0.017	0.053	0.010	<i>INTU</i>	TSS1500		0.0420	0.956
cg10179300	0.876	0.030	0.899	0.022	<i>TRIO</i>	Body	S_Shelf	0.0439	0.956
cg18219562	0.818	0.036	0.845	0.031				0.0499	0.956
cg16151636	0.047	0.007	0.044	0.003	<i>NR4A2</i>	TSS1500	Island	0.0506	0.956
cg00094412	0.619	0.034	0.645	0.035	<i>GABBR1</i>	Body	N_Shelf	0.0556	0.956
cg27247382	0.964	0.008	0.970	0.008	<i>PLEKHM3</i>	3'UTR		0.0557	0.956
cg04292672	0.893	0.015	0.904	0.014	<i>MORNI</i>	Body	N_Shelf	0.0581	0.956
cg10746778	0.526	0.044	0.558	0.041	<i>SORL1</i>	Body		0.0583	0.956
cg11156132	0.779	0.017	0.792	0.018			S_Shelf	0.0612	0.956
cg19990182	0.045	0.005	0.041	0.006	<i>WDR35</i>	TSS200	Island	0.0654	0.956
cg11504355	0.855	0.026	0.873	0.019	<i>KIRREL</i>	3'UTR		0.0695	0.956
cg09204618	0.950	0.008	0.956	0.007	<i>TSSK2</i>	TSS1500	N_Shelf	0.0721	0.956
cg10814005	0.137	0.023	0.122	0.013	<i>GPR68</i>	5'UTR		0.0727	0.956
cg12470014	0.958	0.006	0.963	0.005			N_Shore	0.0793	0.956
cg18030453	0.585	0.036	0.609	0.033	<i>LARS2</i>	Body		0.0803	0.956
cg21525627	0.936	0.013	0.945	0.014				0.0806	0.956

The differentially methylated CpG site, cg19196862, corresponded to the body of the *IGF2R* gene. Cg19196862 (*IGF2R*) exhibited a single peak distribution showing hypermethylated state (Figure 6). The CpGs did not show significant differences in methylation status between 2 and 6 years old.

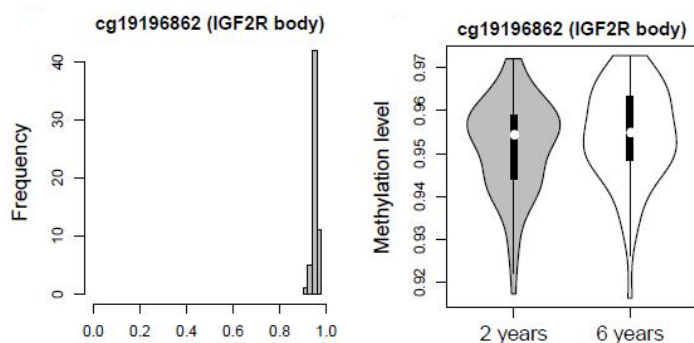


Figure 6. Left: Distribution of methylation levels at cg19196862 (*IGF2R*), Right: Violin plot showing the distribution of methylation levels at age 2 and 6 years at cg19196862 (*IGF2R*)

The cg19196862 (*IGF2R*) of 2-year-old showed a higher DNA methylation levels in the high BPA exposure group compared to the low BPA exposure group. However, this difference between the two groups was not significant at the age of 6 (Figure 7).

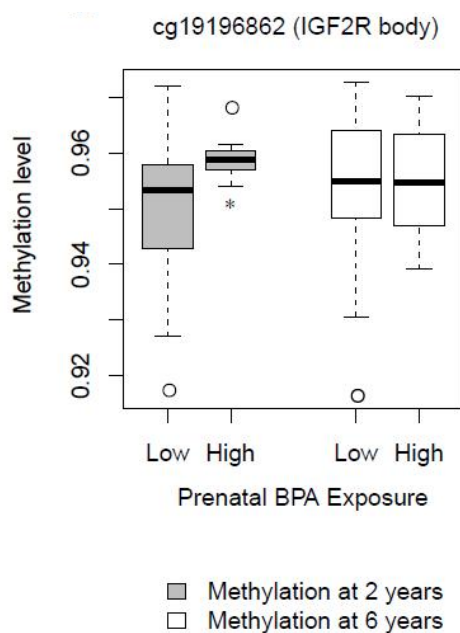


Figure 7. Methylation levels at cg19196862 (*IGF2R*) by prenatal BPA exposure at age 2 and 6 years

Abbreviation: BPA, bisphenol A.

*FDR corrected P-value <0.05

DNA methylation levels at cg19196862 (*IGF2R*) were not different by prenatal BPA exposure when CpG sites at CpG island, 5' untranslated region, transcription start site 200 (TSS200) or TSS1500 were inspected both at ages 2 (Table 8) and 6 (Table 9).

Table 8. Mean DNA methylation levels at age 2 at each CpG site by prenatal bisphenol A exposure levels (high (n=8) vs. low (n=51))(Top 5 CpG sites sorted by p-values at CpG island or promoter regions)

Classification*	CpG site	High prenatal BPA		Low prenatal BPA		UCSC Gene Name	Classification*	p_value	FDR corrected p-value
		Mean	SD	Mean	SD				
CpG island n=101 [†]	cg15913725	0.955	0.011	0.933	0.019	<i>TSSCI</i>	Body	0.014	0.9998
	cg00852675	0.863	0.027	0.882	0.0237	<i>LOC728743</i>	Body	0.059	0.9998
	cg09230763	0.833	0.046	0.801	0.0434	<i>MAP3K6</i>	Body	0.071	0.9998
	cg18330571	0.850	0.029	0.831	0.0305	<i>EBF3</i>	Body	0.091	0.9998
	cg17111837	0.063	0.011	0.056	0.0102	<i>NCRNA00176</i>	Body	0.111	0.9998
5'UTR n=45	cg24217948	0.865	0.044	0.897	0.0242	<i>SETBP1</i>	S_Shore	0.045	0.8116
	cg10814005	0.120	0.024	0.130	0.0096	<i>GPR68</i>		0.063	0.8116
	cg13781414	0.803	0.035	0.826	0.0261	<i>NACC2</i>		0.081	0.8116
	cg14286682	0.814	0.032	0.799	0.0266	<i>TPD52L3</i>		0.244	0.8292
	cg05845030	0.595	0.039	0.579	0.0389	<i>DCN</i>		0.272	0.8292
TSS200 n=39	cg13123009	0.409	0.025	0.388	0.0262	<i>LY6G6E</i>		0.031	0.9613
	cg11245333	0.048	0.010	0.054	0.00506	<i>MOSCI</i>	N_Shore	0.101	0.9613
	cg02244028	0.907	0.025	0.922	0.0188	<i>SCN11A</i>		0.116	0.9613
	cg21584983	0.040	0.006	0.042	0.00334	<i>ECSIT</i>	S_Shore	0.200	0.9613
	cg10054641	0.398	0.047	0.376	0.0322	<i>TMEM71</i>		0.201	0.9613
TSS1500 n=68	cg20117675	0.805	0.031	0.821	0.0132	<i>DHX16</i>	S_Shore	0.016	0.7571
	cg26666886	0.085	0.012	0.094	0.0131	<i>ANKRD11</i>	S_Shore	0.046	0.9103
	cg15059608	0.078	0.012	0.071	0.0115	<i>C3orf14</i>	S_Shore	0.085	0.9103
	cg03523676	0.620	0.041	0.644	0.0259	<i>CPNE6</i>		0.118	0.9103
	cg26687842	0.573	0.040	0.596	0.0523	<i>LOC646982</i>		0.158	0.9103

*UCSC reference gene group or relation to UCSC CpG Island

[†]Number of CpG sites out of the selected 565 CpG sites

Table 9. Mean DNA methylation levels at age 6 at each CpG site by prenatal bisphenol A exposure levels (high (n=12) vs. low (n=49))(Top 5 CpG sites sorted by p-values at CpG island or promoter regions)

Classification*	CpG site	High prenatal BPA		Low prenatal BPA		UCSC Gene Name	Classification*	p_value	FDR corrected p-value
		Mean	SD	Mean	SD				
CpG island n=83 [†]	cg03862225	0.037	0.006	0.033	0.005	<i>CTBP2</i>	TSS1500	0.041	0.9638
	cg16151636	0.047	0.007	0.044	0.003	<i>NR4A2</i>	TSS1500	0.051	0.9638
	cg19990182	0.045	0.005	0.041	0.006	<i>WDR35</i>	TSS200	0.065	0.9638
	cg26317405	0.042	0.009	0.037	0.007	<i>ATPGD1</i>	Body	0.082	0.9638
	cg15913725	0.957	0.011	0.943	0.02	<i>TSSCI</i>	Body	0.087	0.9638
5' UTR n=15	cg10814005	0.137	0.023	0.122	0.013	<i>GPR68</i>		0.073	0.8361
	cg21282997	0.426	0.040	0.449	0.062	<i>IL18RAP</i>		0.163	0.8361
	cg17627898	0.510	0.091	0.553	0.07	<i>TAOK3</i>		0.209	0.8361
	cg18568872	0.608	0.025	0.598	0.027	<i>ZNF710</i>	N_Shelf	0.274	0.8361
	cg13781414	0.829	0.027	0.820	0.027	<i>NACC2</i>		0.376	0.8361
TSS200 n=17	cg08568550	0.882	0.022	0.894	0.021	<i>C11orf16</i>		0.140	0.8967
	cg20587336	0.027	0.005	0.025	0.004	<i>ARMC1</i>	S_Shore	0.282	0.8967
	cg08339192	0.042	0.008	0.045	0.005	<i>SIGLEC14</i>		0.305	0.8967
	cg11245333	0.053	0.014	0.059	0.015	<i>MOSC1</i>	N_Shore	0.305	0.8967
	cg04219544	0.862	0.031	0.873	0.016	<i>KRT24</i>		0.337	0.8967
TSS1500 n=34	cg03523676	0.599	0.036	0.630	0.025	<i>CPNE6</i>		0.021	0.5735
	cg13084458	0.065	0.017	0.053	0.01	<i>INTU</i>		0.042	0.5735
	cg16151636	0.047	0.007	0.044	0.003	<i>NR4A2</i>	Island	0.051	0.5735
	cg09204618	0.950	0.008	0.956	0.007	<i>TSSK2</i>	N_Shelf	0.072	0.5786
	cg02259997	0.042	0.006	0.038	0.006	<i>FGF9</i>	Island	0.093	0.5786

*UCSC reference gene group or relation to UCSC CpG Island

[†]Number of CpG sites out of the selected 565 CpG sites

The association between \log_2 (prenatal BPA) and DNA methylation at cg19196862 (*IGF2R*) was inspected by generalized additive model (GAM) by adjusting for mother's age, BMI, education level, and child's blood cell type fractions, which showed non-linear pattern (J-shape) (Figure 8). The threshold analysis indicated that the first fit had a negative slope (β : -0.00175 (95% CI: -0.00647, 0.00297)) and the second fit had a positive slope (β : 0.00651 (95% CI: 0.000160, 0.0129)) with the threshold point 1.300 in log scale which is equal to 2.462 μ g/g creatinine (Table 10), which corresponds to between 75th and 80th percentile (Table 11).

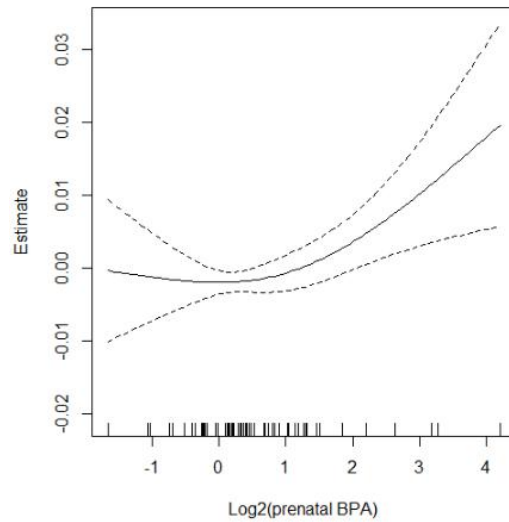


Figure 8. Generalized additive model for the association between $\log_2(\text{prenatal BPA})$ and DNA methylation levels at cg19196862 (IGF2R) adjusted for mother's age, BMI, education, and cell type fractions

Table 10. Threshold point estimation for the non-linear model for the association between $\log_2(\text{prenatal BPA})$ and DNA methylation levels at cg19196862 (IGF2R)

	Estimate (95% CI)	p-value	Threshold point	$2^{1.300}$
Fit 1	-0.00175 (-0.00647, 0.00297)	0.472		
Fit 2	0.00651 (0.000160, 0.0129)	0.0446	1.300	2.462

Table 11. Difference in methylation levels in cg19196862 (IGF2R) in 2-year children by high vs. low prenatal BPA exposures with different cut off values (n=59)

Percentile	Cut off value ($\mu\text{g/g creatinine}$)	Mean methylation levels		p-value from the t-test
		Low prenatal BPA	High prenatal BPA	
75th	2.354	0.950 (N=47)	0.957 (N=12)	0.0174
80th	2.678	0.950 (N=51)	0.959 (N=8)	0.0003
90th	4.244	0.951 (N=53)	0.961 (N=6)	0.0004

Differential methylation levels in children at ages 2 and

6 years according to postnatal BPA exposure

The effects of postnatal BPA on DNA methylation at the selected 594 CpG were also studied. Mean levels of DNA methylations at ages 2, 6, 6, 6 years were inspected by postnatal BPA exposure group at 2, 2, 4, 6 years, respectively (Table 12), in which none was significant (Table 13, 14, 15, and 16).

Table 12. Matching of ages at bisphenol A exposure and ages for DNA methylation in Table 13~16.

	Exposure (BPA)	Outcome (DNA methylation)
Table 11	Age 2	Age 2
Table 12	Age 2	Age 6
Table 13	Age 4	Age 6
Table 14	Age 6	Age 6

Table 13. Mean DNA methylation levels at age 2 at each CpG site by postnatal bisphenol A exposure at age 2 (high (n=6) vs. low (n=25)) (Top 25 CpG sites sorted by p-values)

CpG site	High prenatal BPA		Low prenatal BPA		UCSC Gene Name	UCSC Ref Gene Group	Relati on to UCSC CpG Island	p_value	FDR corre cted p-val ue
	Mean	SD	Mean	SD					
cg08568550	0.848	0.050	0.885	0.012	<i>C11orf16</i>	TSS200		0.0026	0.509
cg27267258	0.938	0.033	0.953	0.007	<i>ANKRD11</i>	Body		0.0414	0.602
cg12170787	0.475	0.124	0.529	0.014	<i>SBNO2</i>	Body		0.0420	0.602
cg17478979	0.493	0.120	0.440	0.023	<i>ZC3H12D</i>	Body	Island	0.0472	0.602
cg02716826	0.497	0.117	0.441	0.042	<i>SUGT1P1</i>	Body	N_Shore	0.0697	0.602
cg13641993	0.933	0.023	0.944	0.007	<i>FBXO10</i>	5'UTR		0.0708	0.602
cg17167536	0.805	0.186	0.875	0.016	<i>XKR6</i>	Body		0.0759	0.602
cg01706498	0.741	0.180	0.810	0.028	<i>KLHL6</i>	Body		0.0774	0.602
cg24217948	0.844	0.093	0.885	0.030	<i>SETBP1</i>	5'UTR	S_Shore	0.0802	0.602
cg26627956	0.922	0.064	0.945	0.007	<i>CFLAR</i>	Body		0.0853	0.602
cg11475880	0.876	0.105	0.924	0.040	<i>IQSEC2</i>	Body	Island	0.0876	0.602
cg17276103	0.930	0.045	0.946	0.005	<i>DDAH1</i>	Body		0.0883	0.602
cg01538605	0.742	0.183	0.813	0.042			N_Shore	0.0892	0.602
cg06882533	0.849	0.204	0.921	0.007				0.0898	0.602
cg03327570	0.828	0.169	0.889	0.020				0.0928	0.602
cg21960828	0.954	0.057	0.974	0.007	<i>TADA2B</i>	Body	Island	0.1012	0.602
cg06437396	0.124	0.131	0.080	0.007			N_Shore	0.1073	0.602
cg23166970	0.114	0.216	0.042	0.009	<i>MCCC1</i>	TSS1500	S_Shore	0.1091	0.602
cg14391148	0.925	0.041	0.938	0.003	<i>C9orf167</i>	3'UTR	Island	0.1101	0.602
cg07570055	0.145	0.233	0.068	0.011			Island	0.1126	0.602
cg10861407	0.947	0.059	0.966	0.004	<i>FSDIL</i>	TSS1500	N_Shore	0.1145	0.602
cg26284544	0.539	0.144	0.594	0.043	<i>SNAPC2</i>	TSS1500	Island	0.1147	0.602
cg02682525	0.643	0.088	0.613	0.017	<i>ANKK1</i>	TSS1500	N_Shore	0.1162	0.602
cg25685359	0.880	0.112	0.917	0.012				0.1180	0.602
cg01172150	0.203	0.193	0.138	0.028			S_Shore	0.1185	0.602

Table 14. Mean DNA methylation levels at age 6 at each CpG site by postnatal bisphenol A exposure at age 2 (high (n=6) vs. low (n=25)) (Top 25 CpG sites sorted by p-values)

CpG site	High prenatal BPA		Low prenatal BPA		UCSC Gene Name	UCSC Ref Gene Group	Relation to UCSC CpG Island	p_value	FDR corrected p-value
	Mean	SD	Mean	SD					
cg06096336	0.535	0.157	0.649	0.046	<i>PSMD1</i>	Body		0.0044	0.651
cg01101459	0.768	0.041	0.720	0.037				0.0134	0.707
cg15416179	0.137	0.073	0.096	0.025	<i>MAP2K3</i>	Body	S_Shore	0.0287	0.707
cg02682525	0.676	0.079	0.635	0.021	<i>ANKKI</i>	TSS1500	N_Shore	0.0304	0.707
cg25178683	0.472	0.111	0.534	0.040	<i>LGALS3BP</i>	TSS1500		0.0340	0.707
cg00585790	0.231	0.177	0.148	0.029	<i>LIMS1</i>	1stExon		0.0354	0.707
cg04836151	0.794	0.076	0.722	0.054				0.0389	0.707
cg17478979	0.414	0.147	0.337	0.049	<i>ZC3H12D</i>	Body	Island	0.0398	0.707
cg02426464	0.260	0.169	0.186	0.026	<i>SLC43A2</i>	Body	S_Shelf	0.0452	0.707
cg03725309	0.392	0.169	0.306	0.059	<i>SARS</i>	Body	S_Shore	0.0480	0.707
cg10802680	0.563	0.153	0.635	0.041	<i>DIABLO</i>	TSS200;	S_Shore	0.0499	0.707
cg05063895	0.239	0.191	0.162	0.019			N_Shelf	0.0573	0.707
cg03746015	0.807	0.041	0.770	0.044	<i>CLEC16A</i>	Body		0.0579	0.707
cg21584983	0.035	0.008	0.042	0.008	<i>ECSIT</i>	TSS200	S_Shore	0.0613	0.707
cg04232128	0.368	0.066	0.315	0.036	<i>TMEM173</i>	Body		0.0704	0.707
cg01172150	0.237	0.174	0.166	0.040			S_Shore	0.0719	0.707
cg04027757	0.914	0.028	0.891	0.020	<i>POM121L1P</i>	TSS200	Island	0.0722	0.707
cg00134210	0.174	0.151	0.109	0.045	<i>FAM107B</i>	Body	N_Shore	0.0768	0.707
cg12170787	0.495	0.127	0.547	0.031	<i>SBNO2</i>	Body		0.0782	0.707
cg05659486	0.771	0.200	0.844	0.021				0.0853	0.707
cg17272620	0.154	0.093	0.115	0.031	<i>LRG1</i>	TSS1500	N_Shelf	0.0932	0.707
cg01538605	0.741	0.185	0.804	0.017			N_Shore	0.1034	0.707
cg17526229	0.219	0.090	0.186	0.023			Island	0.1065	0.707
cg08309687	0.518	0.150	0.573	0.037				0.1121	0.707
cg06376715	0.428	0.112	0.467	0.022	<i>TP73</i>	Body	Island	0.1154	0.707

Table 15. Mean DNA methylation levels at age 6 at each CpG site by postnatal bisphenol A exposure at age 4 (high (n=6) vs. low (n=53)) (Top 25 CpG sites sorted by p-values)

CpG site	High prenatal BPA		Low prenatal BPA		UCSC Gene Name	UCSC Ref Gene Group	Relation to UCSC CpG Island	p_value	FDR corrected p-value
	Mean	SD	Mean	SD					
cg09152259	0.464	0.034	0.416	0.046			N_Shelf	0.0021	0.634
cg01936370	0.522	0.033	0.507	0.007			Island	0.0058	0.996
cg03046925	0.906	0.015	0.923	0.012	<i>TRIM15</i>	Body		0.0106	0.996
cg08877257	0.863	0.027	0.836	0.032	<i>MAZ</i>	Body	S_Shore	0.0262	0.996
cg13274254	0.092	0.017	0.108	0.011	<i>GULP1</i>	5'UTR	Island	0.0273	0.996
cg06372962	0.104	0.016	0.119	0.019	<i>ANKRD45</i>	5'UTR	Island	0.0327	0.996
cg26687842	0.639	0.039	0.674	0.042	<i>LOC646982</i>	TSS1500		0.0431	0.996
cg27115863	0.508	0.025	0.486	0.027				0.0478	0.996
cg20722088	0.931	0.013	0.941	0.008	<i>DUSP6</i>	3'UTR	N_Shelf	0.0738	0.996
cg11475880	0.935	0.022	0.952	0.020	<i>IQSEC2</i>	Body	Island	0.0821	0.996
cg25178683	0.511	0.057	0.553	0.041	<i>LGALS3BP</i>	TSS1500		0.0862	0.996
cg02286155	0.696	0.018	0.710	0.024			N_Shore	0.0884	0.996
cg10044470	0.384	0.029	0.362	0.021				0.0888	0.996
cg22352078	0.065	0.010	0.073	0.012			Island	0.1010	0.996
cg13123009	0.429	0.022	0.445	0.025	<i>LY6G6E</i>	TSS200		0.1037	0.996
cg22012981	0.791	0.025	0.773	0.026	<i>ACOX2</i>	5'UTR		0.1039	0.996
cg12917475	0.132	0.028	0.153	0.038	<i>BCL2L2</i>	TSS1500	S_Shelf	0.1042	0.996
cg19695507	0.107	0.026	0.125	0.037	<i>BEND7</i>	Body		0.1125	0.996
cg02716826	0.427	0.031	0.405	0.045	<i>SUGTIP1</i>	Body;Body	N_Shore	0.1148	0.996
cg19202292	0.089	0.017	0.101	0.017			Island	0.1176	0.996
cg04292672	0.896	0.015	0.885	0.020	<i>MORN1</i>	Body	N_Shelf	0.1197	0.996
cg00585790	0.173	0.043	0.202	0.047	<i>LIMS1</i>	1stExon		0.1226	0.996
cg02729344	0.906	0.020	0.920	0.022			N_Shore	0.1260	0.996
cg07800670	0.905	0.028	0.887	0.034	<i>DST</i>	Body		0.1299	0.996
cg07950000	0.176	0.030	0.197	0.041	<i>GRIK1</i>	TSS200	S_Shore	0.1302	0.996

Table 16. Mean DNA methylation levels at age 6 at each CpG site by postnatal bisphenol A exposure at age 6 (high (n=12) vs. low (n=47)) (Top 25 CpG sites sorted by p-values)

CpG site	High prenatal BPA		Low prenatal BPA		UCSC Gene Name	UCSC Ref Gene Group	Relation to UCSC CpG Island	p_value	FDR corrected p-value
	Mean	SD	Mean	SD					
cg06898549	0.783	0.040	0.824	0.033			N_Shelf	0.0019	0.192
cg27038634	0.421	0.029	0.449	0.026			N_Shore	0.0046	0.263
cg09121516	0.960	0.008	0.967	0.008	<i>TFAP4</i>	Body	S_Shore	0.0053	0.263
cg25178683	0.526	0.051	0.476	0.060	<i>LGALS3BP</i>	TSS1500		0.0054	0.263
cg14524936	0.445	0.051	0.494	0.061	<i>SLC6A5</i>	Body		0.0066	0.280
cg22012981	0.785	0.024	0.806	0.026	<i>ACOX2</i>	5'UTR		0.0092	0.299
cg05596468	0.948	0.011	0.953	0.005	<i>ARHGEF10</i>	Body		0.0112	0.299
cg26164488	0.450	0.079	0.515	0.075				0.0124	0.299
cg02695873	0.594	0.026	0.615	0.022			N_Shelf	0.0134	0.299
cg24751284	0.957	0.009	0.964	0.007	<i>APEX1</i>	Body	S_Shore	0.0152	0.299
cg03012642	0.961	0.016	0.969	0.008				0.0156	0.299
cg19680332	0.256	0.035	0.284	0.036	<i>BCO2</i>	TSS200		0.0156	0.299
cg25001190	0.795	0.038	0.826	0.037	<i>NFIA</i>	Body		0.0156	0.299
cg22078907	0.959	0.006	0.964	0.004	<i>USP22</i>	Body		0.0156	0.299
cg00134210	0.128	0.037	0.157	0.031	<i>FAM107B</i>	Body	N_Shore	0.0168	0.312
cg00634542	0.625	0.030	0.650	0.036	<i>SLC11A1</i>	Body	N_Shore	0.0180	0.312
cg03615565	0.632	0.023	0.653	0.035	<i>FAM65A</i>	Body	Island	0.0187	0.312
cg05063895	0.176	0.021	0.193	0.022			N_Shelf	0.0189	0.312
cg21186778	0.835	0.022	0.852	0.024	<i>RCL1</i>	Body		0.0198	0.312
cg00673344	0.366	0.056	0.407	0.048			S_Shore	0.0243	0.328
cg09245901	0.791	0.028	0.813	0.031				0.0249	0.328
cg26470501	0.556	0.028	0.578	0.039	<i>BCL3</i>	Body	S_Shore	0.0259	0.335
cg15416179	0.119	0.034	0.143	0.032	<i>MAP2K3</i>	Body	S_Shore	0.0288	0.345
cg14524775	0.960	0.007	0.965	0.006	<i>ARHGEF2</i>	Body	Island	0.0294	0.345
cg27117792	0.378	0.068	0.426	0.063				0.0295	0.345
cg22820188	0.478	0.030	0.499	0.020	<i>LMNA</i>	Body	S_Shore	0.0325	0.345
cg03327570	0.773	0.034	0.800	0.050				0.0339	0.348
cg18219562	0.817	0.036	0.842	0.032				0.0348	0.348
cg15650694	0.070	0.010	0.064	0.006	<i>SFRS12</i>	TSS200	Island	0.0354	0.348

Methylation status at age 2 years and child's BMI in early childhood

One standard deviation (SD) change of methylation levels at cg19196862 (*IGF2R*) at age 2 was associated with 0.253 (95% CI; 0.050, 0.456), 0.243 (95% CI; 0.030, 0.455), 0.251 (95% CI; 0.030, 0.472), and 0.322 (95% CI; 0.034, 0.610) increase of BMI Z-score at ages 2, 4, 6, and 8 years (Table 17 and Figure 9), respectively, when adjusted for covariates mentioned in statistical analysis. This association showed interaction effect by sex, where the effect size for the association between methylation at cg19196862 (*IGF2R*) at age 2 years and BMI Z-scores in early childhood was greater in girls than in boys, although sex-difference was significant at only age 6 years. When stratified by sex, the association between methylation at cg19196862 (*IGF2R*) at age 2 years and BMI Z-scores from 2, 4, 6, to 8 years was significant in only girls, by 0.272 (95% CI; 0.011, 0.534) at age 2 years, 0.339 (95% CI; 0.060, 0.617) at age 4 years, 0.437 (95% CI; 0.165, 0.709) at age 6 years, and 0.543 (95% CI; 0.178, 0.908) at age 8 years, showing increasing effect sizes as age increases.

Table 17. Association between methylation at cg19196862 (*IGF2R*) and BMI and BMI Z-score (n=59)

Obesity measure	Age (Years)	Overall		Boys†		Girls†		Sex difference (reference: boys)	
		Estimate* (95% CI)	P-value	Estimate (95% CI)	P-value	Estimate (95% CI)	P-value	Estimate	P-value
BMI	2	0.371 (0.070, 0.673)	0.020*	0.343 (-.133, 0.820)	0.165	0.395 (0.006, 0.785)	0.053	0.023	0.943
	4	0.280 (-.005, 0.566)	0.061	0.081 (-.342, 0.504)	0.710	0.425 (0.051, 0.799)	0.032*	0.337	0.259
	6	0.304 (-.120, 0.728)	0.168	-.283 (-.906, 0.339)	0.378	0.675 (0.157, 1.193)	0.015*	0.982	0.026*
	8	0.662 (-.055, 1.379)	0.079	-.144 (-1.16, 0.868)	0.782	1.245 (0.343, 2.146)	0.010*	1.401	0.053
BMI Z-score	2	0.253 (0.050, 0.456)	0.019*	0.228 (-.092, 0.549)	0.170	0.272 (0.011, 0.534)	0.048*	0.025	0.909
	4	0.243 (0.030, 0.455)	0.031*	0.111 (-.204, 0.427)	0.494	0.339 (0.060, 0.617)	0.022*	0.218	0.328
	6	0.251 (0.030, 0.472)	0.032*	-.041 (-.367, 0.286)	0.809	0.437 (0.165, 0.709)	0.003*	0.481	0.037*
	8	0.322 (0.034, 0.610)	0.035*	0.018 (-.392, 0.428)	0.932	0.543 (0.178, 0.908)	0.006*	0.523	0.073

*Adjusted for mother's age at pregnancy, mother's and father's prepregnant BMI, mother's education level, child's sex, preterm birth or not (<37 weeks), underweight at birth or not (<2500g), breastfeeding for ≥6 months or not, child's urinary BPA(ug/creatinine), child's total calorie intake (kcal), and cell type fraction.

†Estimates for boys and girls were obtained by inserting sex interaction term in the regression analysis.

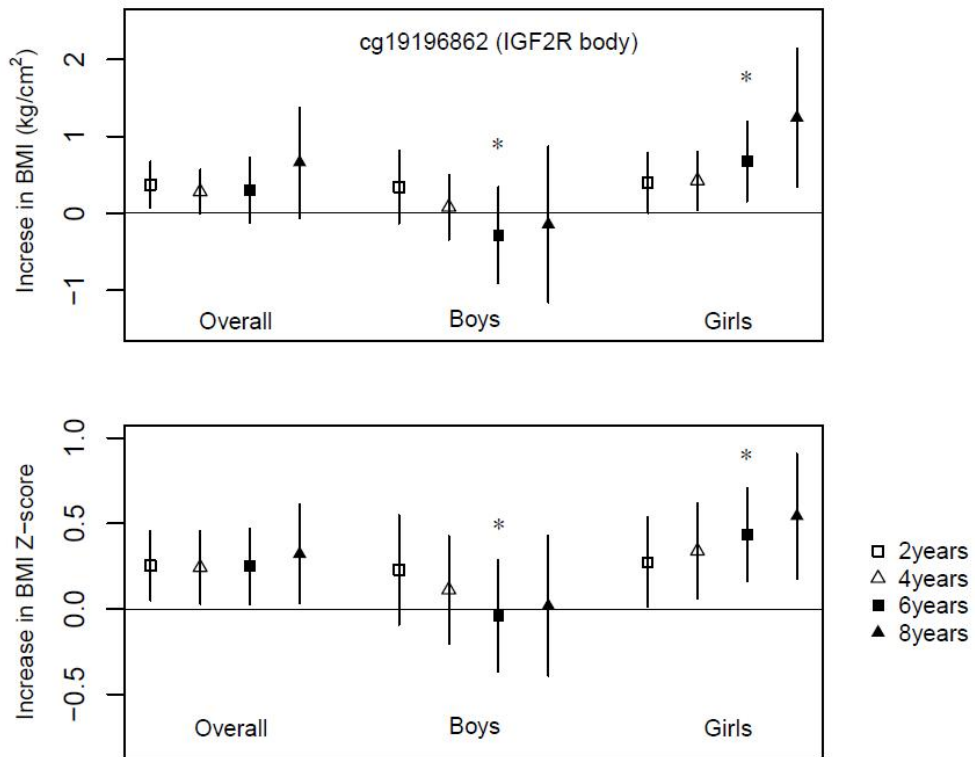


Figure 9. Increase in BMI and BMI Z-score and 95% confidence interval by 1 standard deviation increase of methylation levels at cg19196862 (*IGF2R*)

*Sex difference was significant.

Adjusted by mother's age at pregnancy, mother's and father's BMI, mother's education level, child's sex, preterm birth or not (<37 weeks), underweight at birth or not (<2500g), breastfeeding for ≥ 6 months or not, child's urinary BPA(ug/creatinine), child's total calorie intake (kcal), and cell type fraction...
Abbreviation: BMI, body mass index.

Mediation analysis

The average causal mediation effect of methylation at cg19196862 (*IGF2R*) on the association between prenatal BPA exposure and BMI Z-score in boys and girls overall was 0.064 (p-value 0.058) at age 2, 0.069 (p-value 0.040) at age 4, 0.061 (p-value 0.084) at age 6, and 0.092 (p-value 0.030) at age 8, showing the greatest effect at age 8 (Table 18, Figure 10). The average direct effects were mostly negative, while the total effects were mostly positive.

Table 18. Mediation effect of methylation at cg19196862 (*IGF2R* body) on the association between prenatal BPA exposure and BMI Z-score.

Age	Path	Effect	Estimate	p-value
2 years	a*	Prenatal BPA - child methylation	0.003 (0.001, 2.219)	0.031*
	b*	Methylation - BMI	0.253 (0.050, 0.456)	0.019*
	c*	Average causal mediation effect	0.064 (-0.001, 0.17)	0.058
		Average direct effect	-0.018 (-0.264, 0.23)	0.870
		Total Effect	0.046 (-0.216, 0.32)	0.716
		Proportion Mediated	0.305 (-7.535, 5.94)	0.710
	4 years	a	Prenatal BPA - child methylation	0.003 (0.001, 2.219)
b		Methylation - BMI	0.243 (0.030, 0.455)	0.031*
c		Average causal mediation effect	0.069 (0.002, 0.17)	0.040*
		Average direct effect	-0.136 (-0.4, 0.12)	0.290
		Total Effect	-0.067 (-0.338, 0.2)	0.630
		Proportion Mediated	-0.242 (-9.377, 6.44)	0.650
6 years		a	Prenatal BPA - child methylation	0.003 (0.001, 2.22)
	b	Methylation - BMI	0.251 (0.030, 0.472)	0.032*
	c	Average causal mediation effect	0.061 (-0.004, 0.16)	0.084
		Average direct effect	-0.027 (-0.279, 0.24)	0.862
		Total Effect	0.035 (-0.248, 0.31)	0.814
		Proportion Mediated	0.186 (-7.969, 6.38)	0.806
	8 years	a	Prenatal BPA - child methylation	0.003 (0.001, 2.353)
b		Methylation - BMI	0.322 (0.034, 0.610)	0.035*
c		Average causal mediation effect	0.092 (0.005, 0.22)	0.030*
		Average direct effect	0.083 (-0.304, 0.45)	0.650
		Total Effect	0.176 (-0.206, 0.54)	0.370
		Proportion Mediated	0.328 (-3.225, 4.36)	0.380

*Defined as in Figure 14.

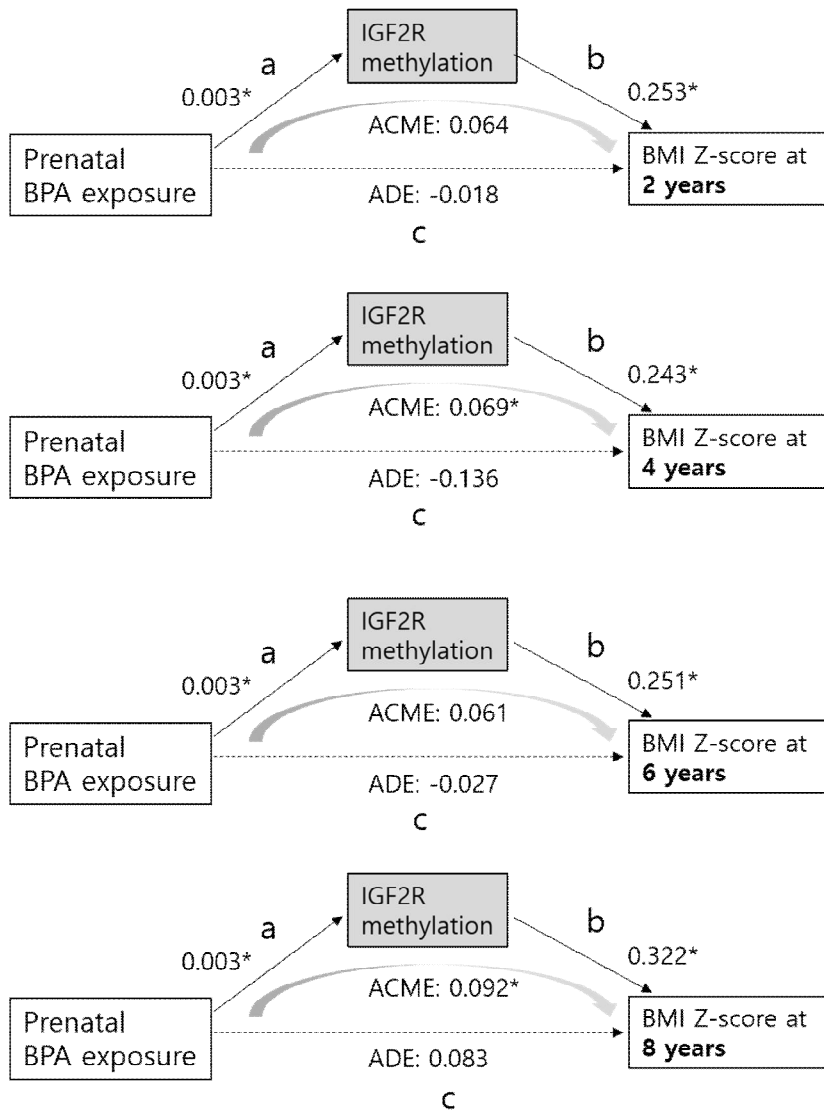


Figure 10. Mediation effect of methylation at cg19196862 (*IGF2R*) on the association between prenatal BPA exposure and BMI Z-score in boys and girls overall.

a: association between prenatal BPA exposure and methylation at cg19196862 (*IGF2R*). b: association between methylation at cg19196862 (*IGF2R*) and BMI Z-score

*P-value <0.05. Abbreviation: BMI, body mass index; BPA, bisphenol A.

Sensitivity analysis

In the sensitivity analysis, in addition to the covariates included in the main analysis, a linear regression analysis was performed on the methylation levels of cg19196862 (*IGF2R*) sites and their association with BMI and BMI Z-scores after additional adjustments for multiple birth, smoking, and drinking. Significance levels changed, but the patterns were similar for cg19196862 (Table 19, Figure 11).

To assess the risk of over-fitting due to adjusting for many covariates, R^2 was checked (Supplementary Table 2). Instead, the propensity score was solely adjusted for the linear regression analysis for DNA methylation and BMI or BMI Z-score. Although R^2 decreased (Supplementary Table 3), the patterns and significance level were similar as in the main analysis (Table 22).

Table 19. Sensitivity analysis for the association between methylation at cg19196862 (*IGF2R*) in 2-year children and increase in BMI and BMI Z-score (n=59)

Obesity measures	Age (Years)	Overall		Boys†		Girls†		Sex difference (reference: girls)	
		Estimate* (95% CI)	P-value	Estimate (95% CI)	P-value	Estimate (95% CI)	P-value	Estimate	P-value
BMI	2	0.404 (0.005, 0.804)	0.0577	0.699 (0.061, 1.337)	0.042*	0.255 (-.240, 0.751)	0.322	-0.502	0.246
	4	0.217 (-.162, 0.596)	0.2724	0.209 (-.377, 0.796)	0.4908	0.226 (-.281, 0.732)	0.3912	-0.001	0.998
	6	0.265 (-.270, 0.801)	0.3411	-.152 (-.998, 0.694)	0.728	0.523 (-.165, 1.210)	0.1499	0.687	0.249
	8	0.391 (-.522, 1.304)	0.4109	-.657 (-1.92, 0.611)	0.3219	1.224 (0.054, 2.394)	0.0537	1.935	0.0499*
BMI Z-score	2	0.276 (0.004, 0.548)	0.0573	0.463 (0.027, 0.899)	0.048*	0.182 (-.157, 0.521)	0.3029	-0.320	0.278
	4	0.198 (-.082, 0.477)	0.1782	0.198 (-.234, 0.630)	0.3786	0.201 (-.173, 0.574)	0.3033	-0.014	0.963
	6	0.239 (-.034, 0.511)	0.0986	0.048 (-.385, 0.481)	0.8309	0.359 (0.007, 0.711)	0.0578	0.307	0.313
	8	0.223 (-.148, 0.595)	0.2521	-.177 (-.700, 0.346)	0.5147	0.542 (0.060, 1.025)	0.040*	0.734	0.069

*Adjusted for mother's age at pregnancy, mother's and father's prepregnant BMI, mother's education level, child's sex, preterm birth or not (<37 weeks), underweight at birth or not (<2500g), breastfeeding for ≥ 6 months or not, child's urinary BPA(ug/creatinine), child's total calorie intake (kcal), and cell type fraction. Additionally adjusted for twin (twin or not), smoking during pregnancy (smoked during pregnancy, did not smoke during pregnancy but smoked before pregnancy, never smoked), and drinking during pregnancy (drank during pregnancy, did not drink during pregnancy but drank before pregnancy, never drank)

†Estimates for boys and girls were obtained by inserting sex interaction term in the regression analysis.

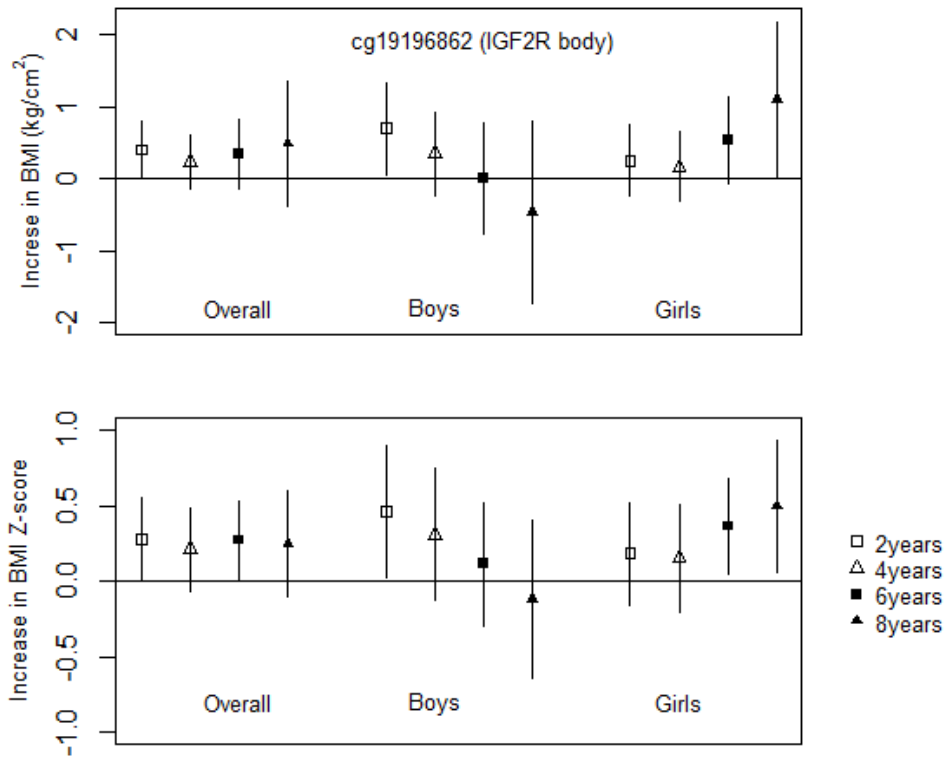


Figure 11. Sensitivity analysis for the increase in BMI and BMI Z-score and 95% confidence interval by 1 standard deviation increase of methylation levels at cg19196862 (*IGF2R*)

Adjusted for mother's age at pregnancy, mother's and father's BMI, mother's education level, child's sex, preterm birth or not (<37 weeks), underweight at birth or not (<2500g), breastfeeding for ≥ 6 months or not, child's urinary BPA(ug/creatinine), child's total calorie intake (kcal), and cell type fraction and additionally twin (or not), smoking during pregnancy (smoked, former smoker, never smoker) and alcohol.

Abbreviation: BMI, body mass index

Table 20. Sensitivity analysis: Association between methylation level (high 50 percentile vs. low 50 percentile) at cg19196862 (*IGF2R*) and BMI and BMI Z-score adjusting for propensity scores (n=59)

Obesity measures	Age (Years)	Overall		Boys†		Girls†		Sex difference (reference: boys)	
		Estimate* (95% CI)	P-value	Estimate (95% CI)	P-value	Estimate (95% CI)	P-value	Estimate	P-value
BMI	2	0.467 (-0.255, 1.188)	0.201	-0.095 (-1.142, 0.954)	0.854	1.009 (-0.003, 2.020)	0.051	0.816	0.189
	4	0.584 (-0.076, 1.244)	0.082	0.133 (-0.750, 1.017)	0.758	1.117 (0.088, 2.146)	0.034*	0.661	0.263
	6	0.619 (-0.388, 1.626)	0.223	-0.181 (-1.733, 1.371)	0.812	1.413 (0.009, 2.817)	0.049*	1.400	0.125
	8	1.306 (-0.183, 2.795)	0.084	-0.179 (-2.628, 2.270)	0.881	2.623 (0.786, 4.459)	0.007*	2.274	0.092
BMI Z-score	2	0.328 (-0.917, 0.393)	0.429	-0.063 (-0.748, 0.623)	0.852	0.704 (0.025, 1.383)	0.043*	0.563	0.172
	4	0.517 (0.0247, 1.010)	0.040*	0.211 (-0.453, 0.876)	0.518	0.892 (0.130, 1.654)	0.023*	0.435	0.322
	6	0.483 (-0.947, 0.629)	0.076	0.038 (-0.736, 0.811)	0.621	0.933 (0.157, 1.709)	0.020*	0.763	0.112
	8	0.683 (0.087, 1.281)	0.026*	0.075 (-0.890, 1.041)	0.325	1.230 (0.502, 1.958)	0.002*	0.933	0.081

*Adjusted for a propensity score created from mother's age at pregnancy, mother's and father's prepregnant BMI, mother's education level, child's sex, preterm birth or not (<37 weeks), underweight at birth or not (<2500g), breastfeeding for ≥6 months or not, child's urinary BPA(ug/creatinine), child's total calorie intake (kcal), and cell type fraction.

†Estimates for boys and girls were obtained by inserting sex interaction term in the regression analysis.

Discussion

DNA methylation in cg19196862, corresponding to the *IGF2R* gene body differed significantly by prenatal BPA exposure at 2 years of age, but not at 6 years of age. The association between methylation at cg19196862 (*IGF2R*) was positive only in girls at 2, 4, 6 and 8 years old and the effect sizes increased with age, but was not significant for boys of any age.

Epigenetic dysregulation has been suggested as one of the mechanisms of the Developmental Origin of Health and Disease (DOHaD) hypothesis. The DOHaD hypothesis shows that environmental stimuli affect growth pathways during critical periods of prenatal and postnatal mammalian development, leading to permanent changes in metabolism and disease susceptibility (Waterland and Michels 2007). In embryonic fertilized cells, DNA methylation is almost completely erased through epigenetic reprogramming in the early stages of the embryo (Kundakovic and Jaric 2017; Smith et al. 2014). Cell-specific DNA methylation is re-established according to the epigenetic profile inherited from parents (epigenetic programming). Epigenetic marks are stabilized in the later stages of development, but are still actively involved in gene expression in the later stages of cell differentiation.

Previous longitudinal methylation studies in children have shown that the methylation profile has changed more dramatically in early childhood than later ages. The methylation status of the 783,659 CpG sites in the blood changed at the 110,726 CpG sites from 0 to 5 years of age, but only 460 CpG sites changed from 5 to 10 years (Perez et al. 2019). Also, there may be a sensitive window period in which the methylation profile changes according to childhood adversity rather than continuous methylation changes over time. For example, changes in DNA methylation

was explained more effectively by adversity in infancy (under 2 years of age) rather than recent adversity (Dunn et al. 2019). In particular, this study showed that prenatal BPA had effects on DNA methylation at early childhood, but postnatal BPA exposure in early childhood had no effects on DNA methylation in children, suggesting that prenatal BPA exposure had a greater impact on DNA methylation than postnatal BPA exposure specifically in respect of *IGF2R*.

In this study, DNA methylation level at cg19196862 (*IGF2R*) varied with prenatal BPA levels at 2 years of age, but no difference was found at 6 years of age. This finding suggests that prenatal toxicity exposure may affect DNA methylation in infancy, but the effect is mitigated as the methylation profile becomes stabilized as the child grows. Additionally, this mitigation would be also due to the fact that more diverse biological and sociological factors come into play in determining obesity in children as they grow older. Nonetheless, it is important to point out that, since DNA methylation profiles become less labile as children grow older, the epigenetic profile set in infancy in regards with prenatal environmental exposure is likely to be sustained over children's growth. Permanent epigenetic changes induced by prenatal exposure would possibly lead to metabolic diseases in later life as in DOHaD hypothesis.

More importantly, epigenetic patterns set in the early developmental period are inherited to the next generation, because epigenetic reprogramming takes place by copying parental epigenetic profiles (Kundakovic and Jaric 2017). Previous studies showed that epigenetic marks induced by specific maternal environmental exposures during pregnancy were inherited to multiple generations of descendants even when the exposure was absent. For example, male rats born to mothers exposed to endocrine

disruptor vinclozolin showed decreased spermatogenic capacity and raised male infertility, which was transferred to 4 subsequent generations (Anway et al. 2005). These effects were correlated with DNA methylation patterns. Thus, maternal exposure to environmental toxic chemicals may not only contribute to permanent epigenetic marks in children leading to effects on health and diseases in their later lives but also leave epigenetic marks on the next generations.

IGF2 is known for genomic imprinting, which refers to parent-of-origin-dependent allele-specific gene expression in which gene expression occurs only from mother (maternally imprinted) or from father (paternally imprinted). However, in human, *IGF2R* showed non-imprinted biallelic expression (Buckberry et al. 2012; Oudejans et al. 2001; Vu et al. 2006). Cg19196862 is located at the 31st exon of *IGF2R*. *IGF2R* regulates *IGF2* by binding to it, internalizing and transporting it to the lysosome for degradation (Hassan 2003). Thus, *IGF2R* represses the expression of *IGF2* by reducing its concentration. A previous study showed a negative association between methylation at *IGF2* and BMI in children (Do et al. 2019). It could be postulated that the greater methylation at *IGF2R* results in a lesser degree of *IGF2R* expression, leading to an increased level of IGF2 increasing obese tendency. However, the specific direction of the relationship between methylation and gene expression should be confirmed by mRNA expression studies in the future.

The reasons for sex-specific obesogenic effects of BPA are not clear. The associations between prenatal BPA exposure and body size were null in previous studies (Braun et al. 2014; Philippat et al. 2014) but it was positive (Valvi et al. 2013) or negative in girls only (Harly et al. 2013). The differences among studies could be due to the timing of measurement,

age at outcome assessment, or differences in population susceptibility (Buckley, 2016). Phenols, including BPA, are endocrine-disrupting chemicals that alter metabolism via estrogenic, antiestrogenic, or anti-androgenic activities and may interfere with hormone functions. Sex-specific effects of BPA could be due to different body composition of fat mass and lean body mass (Hoepner 2106), and/or different sensitivity to estrogenic activity of BPA between boys and girls (van Esterik et al. 2014).

The strength of this study is that it used longitudinal sets of methylation data of children at age 2 and 6 and longitudinal data of obesity measures including BMI and BMI Z-score at ages 2, 4, 6, and 8. This enabled the finding of a sensitive window period of prenatal effects on a child's methylation patterns in early childhood, and the temporal relationships between DNA methylation patterns and obesity outcomes. For example, DNA methylations at *IGF2R* were different by prenatal BPA exposure at age 2 but not at age 6, and DNA methylation status at *IGF2R* at age 2 was associated with BMI at ages 2, 4, 6, and 8 in a sex-dependent manner, reducing the possibility of reverse causation, thus inferring causality.

Second, the information on various covariates were available to control for the analysis of associations between methylation and child's phenotypes. Covariates such as a child's BPA exposure levels and child's dietary information (e.g. total calorie intakes) were available at age 4, 6, and 8, which were adjusted at each age correspondingly.

This study has several limitations. First, the sample size was small. Replication study with a larger sample size is warranted to confirm the epigenetic effects of *IGF2R*.

Second, covariates could not be considered in the t-test for comparisons of DNA methylation by prenatal BPA exposure level. However,

the association between prenatal BPA and methylation at cg19196862 (*IGF2R*) was non-linear when adjusted for mother's age, BMI, education level, and cell type fractions.

Third, for the association between DNA methylation at cg19196862 (*IGF2R*), postnatal BPA was not adjusted at ages 2 due to several missing values, while postnatal BPA were adjusted at ages 4, 6, and 8. Increase in methylation at cg19196862 (*IGF2R*) was associated with increased BMI at ages 2, 4, 6, and 8 with greater effect sizes as age increased. Since BMI at age 2 may not reflect the effects of DNA methylation at age 2, the association between DNA methylation at age 2 and BMI at ages 4, 6, and 8 may be more important.

Forth, information for *IGF2R* gene expression was unavailable. There are many other steps to consider the effect of methylation of CpG sites on obesity. Caution is needed when interpreting the result that *IGF2R* hypermethylation is associated with an increase in the BMI Z-score because the extent of *IGF2R* expression is unknown in this study. The assessment of the impact of *IGF2R* on growth and development through *IGF2* and the effect of methylation of *IGF2R* on the level of IGF2 expression is necessary for future studies.

Fifth, tissue specificity was limited. Blood tissues are comprised of different types of cells, such as CD8+ T cells, CD4+ T cells, natural killer (NK) cells, B cells, monocytes, and neutrophils. Although the cell type fractions were estimated by Houseman's method (2012), the method is based on adult's samples; thus, it may not reflect child's cell type fractions.

Sixth, since candidate gene analysis was performed instead of EWAS, novel CpG sites related to BPA exposure or obesity could have been missed.

Conclusion

In utero exposure to BPA has been indicated as an obesogen in children. From previous obesity-related EWAS, 594 CpG sites were selected and inspected for the association with prenatal BPA exposure levels. The association between methylation at the *IG2R* and obesity were evaluated in children. Methylation at *IGF2R* differed by maternal BPA exposure at age 2 but not at age 6, and was positively associated with BMI Z-score at age 2, 4, 6, and 8 in a sex-dependent manner. DNA methylation levels at 594 CpG sites did not differ by postnatal BPA exposure.

References

- Al Muftah WA, Al-Shafai M, Zaghlool SB, Visconti A, Tsai PC, Kumar P, et al. 2016. Epigenetic associations of type 2 diabetes and BMI in an Arab population. *Clinical Epigenetics* 8:13.
- Anway MD, Cupp AS, Uzumcu M, Skinner MK. 2005. Epigenetic transgenerational actions of endocrine disruptors and male fertility. *Science* 308:1466-1469.
- Aryee MJ, Jaffe AE, Corrada-Bravo H, Ladd-Acosta C, Feinberg AP, Hansen KD, et al. 2014. Minfi: A flexible and comprehensive bioconductor package for the analysis of Infinium DNA methylation microarrays. *Bioinformatics* 30:1363-1369.
- Aslibekyan S, Demerath EW, Mendelson M, Zhi D, Guan W, Liang L, et al. 2015. Epigenome-wide study identifies novel methylation loci associated with body mass index and waist circumference. *Obesity (Silver Spring, Md)* 23:1493-1501.
- Balakrishnan B, Henare K, Thorstensen EB, Ponnampalam AP, Mitchell MD. 2010. Transfer of bisphenol A across the human placenta. *American Journal of Obstetrics and Gynecology* 202:393.e391-397.
- Benjamini Y, Hochberg Y. 1995. Controlling the false discovery rate: A practical and powerful approach to multiple testing. *Journal of the Royal Statistical Society: Series B* 57:289-300.
- Braun JM, Lanphear BP, Calafat AM, Deria S, Khoury J, Howe CJ, et al. 2014. Early-life bisphenol A exposure and child body mass index: A prospective cohort study. *Environmental Health Perspectives* 122:1239-1245.
- Braun JM. 2017. Early-life exposure to EDCs: Role in childhood obesity and neurodevelopment. *Nature Reviews Endocrinology* 13:161-173.

- Buckberry S, Bianco-Miotto T, Hiendleder S, Roberts CT. 2012. Quantitative allele-specific expression and DNA methylation analysis of h19, igf2 and igf2r in the human placenta across gestation reveals h19 imprinting plasticity. *PloS One* 7:e51210.
- Buckley JP, Herring AH, Wolff MS, Calafat AM, Engel SM. 2016. Prenatal exposure to environmental phenols and childhood fat mass in the Mount Sinai children's environmental health study. *Environment International* 91:350-356.
- Calafat AM, Kuklennyik Z, Reidy JA, Caudill SP, Ekong J, Needham LL. 2005. Urinary concentrations of bisphenol A and 4-nonylphenol in a human reference population. *Environmental Health Perspectives* 113:391-395.
- Campanella G, Gunter MJ, Polidoro S, Krogh V, Palli D, Panico S, et al. 2018. Epigenome-wide association study of adiposity and future risk of obesity-related diseases. *International Journal of Obesity (2005)* 42:2022-2035.
- Demerath EW, Guan W, Grove ML, Aslibekyan S, Mendelson M, Zhou YH, et al. 2015. Epigenome-wide association study (EWAS) of BMI, BMI change and waist circumference in African American adults identifies multiple replicated loci. *Human Molecular Genetics* 24:4464-4479.
- Dhana K, Braun KVE, Nano J, Voortman T, Demerath EW, Guan W, et al. 2018. An epigenome-wide association study of obesity-related traits. *American Journal of Epidemiology* 187:1662-1669.
- Do EK, Zucker NL, Huang ZY, Schechter JC, Kollins SH, Maguire RL, et al. 2019. Associations between imprinted gene differentially methylated regions, appetitive traits and body mass index in children. *Pediatric Obesity* 14, e12454.
- Dunn EC, Soare TW, Zhu Y, Simpkin AJ, Suderman MJ, Klengel T, et al.

2019. Sensitive periods for the effect of childhood adversity on DNA methylation: Results from a prospective, longitudinal study. *Biological Psychiatry* 85:838-849.
- Goodrich JM, Dolinoy DC, Sanchez BN, Zhang Z, Meeker JD, Mercado-Garcia A, et al. 2016. Adolescent epigenetic profiles and environmental exposures from early life through peri-adolescence. *Environmental Epigenetics* 2:1-12.
- Harley KG, Aguilar Schall R, Chevrier J, Tyler K, Aguirre H, Bradman A, et al. 2013. Prenatal and postnatal bisphenol A exposure and body mass index in childhood in the CHAMASCOS Cohort. *Environmental Health Perspectives* 121:514-520.
- Hassan AB. 2003. Keys to the hidden treasures of the mannose 6-phosphate/insulin-like growth factor 2 receptor. *The American Journal of Pathology* 162:3-6.
- Hoepner LA, Whyatt RM, Widen EM, Hassoun A, Oberfield SE, Mueller NT, et al. 2016. Bisphenol A and adiposity in an inner-city birth cohort. *Environmental Health Perspectives* 124:1644-1650.
- Houseman EA, Accomando WP, Koestler DC, Christensen BC, Marsit CJ, Nelson HH, et al. 2012. DNA methylation arrays as surrogate measures of cell mixture distribution. *BMC Bioinformatics* 13:86.
- Huang RC, Garratt ES, Pan H, Wu Y, Davis EA, Barton SJ, et al. 2015. Genome-wide methylation analysis identifies differentially methylated CpG loci associated with severe obesity in childhood. *Epigenetics* 10:995-1005.
- Junge KM, Leppert B, Jahreis S, Wissenbach DK, Feltens R, Grutzmann K, et al. 2018. MEST mediates the impact of prenatal bisphenol A exposure on long-term body weight development. *Clinical Epigenetics* 10:58.
- Kim KN, Lim YH, Shin CH, Lee YA, Kim BN, Kim JI, et al. 2018. Cohort profile: The Environment and Development of Children (EDC)

- study: A prospective children's cohort. *International Journal of Epidemiology* 47:1049-1050f.
- Korea Ministry of Environment. 2019. National Environmental Health Survey DB. <https://www.data.go.kr/data/3075219/fileData.do>. Accessed on Dec 10, 2020.
- Kundakovic M, Jaric I. 2017. The epigenetic link between prenatal adverse environments and neurodevelopmental disorders. *Genes (Basel)* 8:3.
- Kvaloy K, Page CM, Holmen TL. 2018. Epigenome-wide methylation differences in a group of lean and obese women - A HUNT Study. *Scientific Reports* 8:16330.
- Lim YH, Bae S, Kim BN, Shin CH, Lee YA, Kim JI, et al. 2017. Prenatal and postnatal bisphenol A exposure and social impairment in 4-year-old children. *Environmental Health* 16:79.
- Lin X, Lim IY, Wu Y, Teh AL, Chen L, Aris IM, et al. 2017. Developmental pathways to adiposity begin before birth and are influenced by genotype, prenatal environment and epigenome. *BMC Medicine* 15:50.
- Miyawaki J, Sakayama K, Kato H, Yamamoto H, Masuno H. 2007. Perinatal and postnatal exposure to bisphenol A increases adipose tissue mass and serum cholesterol level in mice. *Journal of Atherosclerosis and Thrombosis* 14:245-252.
- Moon JS, Lee SY, Nam CM, Choi JM, Choe BK, Weo JW, et al. 2008. 2007 Korean national growth charts: Review of developmental process and an outlook. *Korean Journal of Pediatrics* 51:1-25.
- Myridakis A, Fthenou E, Balaska E, Vakinti M, Kogevinas M, Stephanou EG. 2015. Phthalate esters, parabens and bisphenol-A exposure among mothers and their children in Greece (RHEA Cohort). *Environment International* 83:1-10.
- Oudejans CB, Westerman B, Wouters D, Gooyer S, Leegwater PA, van

- Wijk IJ, et al. 2001. Allelic *IGF2R* repression does not correlate with expression of antisense RNA in human extraembryonic tissues. *Genomics* 73:331-337.
- Perez RF, Santamarina P, Tejedor JR, Urdinguio RG, Alvarez-Pitti J, Redon P, et al. 2019. Longitudinal genome-wide DNA methylation analysis uncovers persistent early-life DNA methylation changes. *Journal of Translational Medicine* 17:15.
- Philippat C, Botton J, Calafat AM, Ye X, Charles MA, Slama R, et al. 2014. Prenatal exposure to phenols and growth in boys. *Epidemiology* 25:625-635.
- Romano ME, Webster GM, Vuong AM, Thomas Zoeller R, Chen A, Hoofnagle AN, et al. 2015. Gestational urinary bisphenol a and maternal and newborn thyroid hormone concentrations: The HOME Study. *Environmental Research* 138:453-460.
- Rzehak P, Covic M, Saffery R, Reischl E, Wahl S, Grote V, et al. 2017. DNA-methylation and body composition in preschool children: Epigenome-wide-analysis in the European childhood obesity project (CHOP)-Study. *Scientific Reports* 7:14349.
- Sayols-Baixeras S, Subirana I, Fernandez-Sanles A, Senti M, Lluís-Ganella C, Marrugat J, et al. 2017. DNA methylation and obesity traits: An epigenome-wide association study. The REGICOR Study. *Epigenetics* 12:909-916.
- Sharp GC, Lawlor DA, Richmond RC, Fraser A, Simpkin A, Suderman M, et al. 2015. Maternal pre-pregnancy BMI and gestational weight gain, offspring DNA methylation and later offspring adiposity: Findings from the AVON longitudinal study of parents and children. *International Journal of Epidemiology* 44:1288-1304.
- Sharp GC, Salas LA, Monnereau C, Allard C, Yousefi P, Everson TM, et

- al. 2017. Maternal BMI at the start of pregnancy and offspring epigenome-wide DNA methylation: Findings from the Pregnancy and Childhood Epigenetics (PACE) Consortium. *Human Molecular Genetics* 26:4067-4085.
- Smith ZD, Chan MM, Humm KC, Karnik R, Mekhoubad S, Regev A, et al. 2014. DNA methylation dynamics of the human preimplantation embryo. *Nature* 511:611-615.
- Taylor JA, Shioda K, Mitsunaga S, Yawata S, Angle BM, Nagel SC, et al. 2018. Prenatal exposure to bisphenol A disrupts naturally occurring bimodal DNA methylation at proximal promoter of *fggy*, an obesity-relevant gene encoding a carbohydrate kinase, in gonadal white adipose tissues of *cd-1* mice. *Endocrinology* 159:779-794.
- Teschendorff AE, Marabita F, Lechner M, Bartlett T, Tegner J, Gomez-Cabrero D, et al. 2013. A beta-mixture quantile normalization method for correcting probe design bias in Illumina Infinium 450K DNA methylation data. *Bioinformatics* 29:189-196.
- Vafeiadi M, Roumeliotaki T, Myridakis A, Chalkiadaki G, Fthenou E, Dermitzaki E, et al. 2016. Association of early life exposure to bisphenol A with obesity and cardiometabolic traits in childhood. *Environmental Research* 146:379-387.
- Valvi D, Casas M, Mendez MA, Ballesteros-Gomez A, Luque N, Rubio S, et al. 2013. Prenatal bisphenol A urine concentrations and early rapid growth and overweight risk in the offspring. *Epidemiology (Cambridge, Mass)* 24:791-799.
- van Esterik JC, Dolle ME, Lamoree MH, van Leeuwen SP, Hamers T, Legler J, et al. 2014. Programming of metabolic effects in *c57bl/6jxfvb* mice by exposure to bisphenol A during gestation and lactation. *Toxicology* 321:40-52.

- van Esterik JC, Vitins AP, Hodemaekers HM, Kamstra JH, Legler J, Pennings JL, et al. 2015. Liver DNA methylation analysis in adult female c57bl/6jxfvb mice following perinatal exposure to bisphenol A. *Toxicology Letters* 232:293-300.
- Vandenberg LN, Hauser R, Marcus M, Olea N, Welshons WV. 2007. Human exposure to bisphenol A (BPA). *Reproductive Toxicology* (Elmsford, NY) 24:139-177.
- Vandenberg LN, Chahoud I, Heindel JJ, Padmanabhan V, Paumgarten FJ, Schoenfelder G. 2010. Urinary, circulating, and tissue biomonitoring studies indicate widespread exposure to bisphenol A. *Environmental Health Perspectives* 118:1055-1070.
- von Goetz N, Wormuth M, Scheringer M, Hungerbuhler K. 2010. Bisphenol A: How the most relevant exposure sources contribute to total consumer exposure. *Risk Analysis* 30:473-487.
- Vu TH, Jirtle RL, Hoffman AR. 2006. Cross-species clues of an epigenetic imprinting regulatory code for the *IGF2R* gene. *Cytogenetic and Genome Research* 113:202-208.
- Wahl S, Drong A, Lehne B, Loh M, Scott WR, Kunze S, et al. 2017. Epigenome-wide association study of body mass index, and the adverse outcomes of adiposity. *Nature* 541:81-86.
- Waterland RA, Michels KB. 2007. Epigenetic epidemiology of the developmental origins hypothesis. *Annual Review of Nutrition* 27:363-388.
- Wilson LE, Harlid S, Xu Z, Sandler DP, Taylor JA. 2017. An epigenome-wide study of body mass index and DNA methylation in blood using participants from the Sister Study Cohort. *International Journal of Obesity* (2005) 41:194-199.
- Xu K, Zhang X, Wang Z, Hu Y, Sinha R. 2018. Epigenome-wide association analysis revealed that *SOCS3* methylation influences the effect

- of cumulative stress on obesity. *Biological Psychology* 131:63-71.
- Yang M, Kim SY, Lee SM, Chang SS, Kawamoto T, Jang JY, et al. 2003. Biological monitoring of bisphenol A in a Korean population. *Archives of Environmental Contamination and Toxicology* 44:546-551.
- Zaghlool SB, Al-Shafai M, Al Muftah WA, Kumar P, Gieger C, Waldenberger M, et al. 2016. Mendelian inheritance of trimodal CpG methylation sites suggests distal cis-acting genetic effects. *Clinical Epigenetics* 8:124.
- Zhang Z, Zheng C, Kim C, Poucke SV, Lin S, Lan P. Causal mediation analysis in the context of clinical research. *Annals of Translational Medicine*. 2016;4(21):425.

초록

산모의 비스페놀 A(bisphenol A) 노출이 후성유전학적 기전을 통해 소아의 비만에 미치는 영향

서울대학교 대학원

의학과 예방의학 전공

최 윤 정

배경: 비스페놀 A는 폴리카보네이트와 같은 열가소성 플라스틱 제조 시 사용되며 전세계에서 가장 많이 쓰이는 화학물질 중 하나로 내분비교란물질로 알려져 있다. 산모의 비스페놀 A 노출이 소아 비만과 관련이 있다는 것은 많은 연구들을 통해 널리 알려져 있다. 이에 DNA 메틸레이션과 같은 후성유전학적 기전이 관여할 것이라는 가설이 제기되었으나 사람 연구에서 근거는 부족하다. 특히 비스페놀 A의 영향은 소아의 성별에 따라 다르다고 알려져 있는데 이와 관련한 후성유전학적 근거는 아직 찾아보기 어렵다.

목표: 본 연구에서는 산모의 비스페놀 노출 및 출생 후 비스페놀 A 노출에 따라 소아의 DNA 메틸레이션에 차이가 나는지 살펴보고, DNA 메틸레이션이 소아의 비만과 관련성이 있는지, 또 성별에 따라 그 영향이 다른지 분석하고자 하였다.

방법: 어린이 환경과 건강(EDC) 코호트에 참여하고 있는 59명의 소아에서 2세와 6세에 반복하여 전혈에서 Infinium HumanMethylation BeadChip을 이용한 전장유전체 수준의 DNA 메틸레이션 분석을 시행하였다. 비

만과 관련된 후성유전체 연관 분석 연구에 대한 문헌고찰을 통해 비만 관련 CpG site 594개를 선별하였다. 산모의 비스페놀 A 노출(80 백분위수 이상 vs. 80 백분위수 미만)에 따라 자녀의 2세 및 6세 전혈 시료 중 594개의 CpG site의 DNA 메틸레이션 수준에 차이가 나는지 분석하였다. 또한 출생 후 2, 4, 6세 시의 비스페놀 A 노출이 2세 및 6세 DNA 메틸레이션에 영향을 주는지 분석하였다. 다음으로 산모의 비스페놀 A 노출과 연관된 CpG site의 DNA 메틸레이션 수준이 소아의 2, 4, 6, 8세 시의 체질량지수(BMI, BMI Z-score)와 관련이 있는지 분석하였다.

결과: 2세 소아 전혈 시료에서 산모의 비스페놀 A 고노출군에서 저노출군에 비해 인슐린 유사 성장인자 2 수용체(*IGF2R*)의 코딩부위인 cg19196862의 메틸레이션 수준이 더 높았다(p-value 0.00030, 위발견율(FDR) 보정 p-value <0.05). 6세에서는 이와 같은 차이가 발견되지 않았다. 2세와 6세 DNA methylation은 출생 후 2, 4, 6세 시의 비스페놀 A 노출 수준과 관련이 없었다. 2세에서 cg19196862의 메틸레이션 수준의 1 표준편차(SD) 증가 시 소아의 2, 4, 6, 8세의 BMI Z-score는 다음과 같아 연령 증가에도 지속적으로 체질량 지수에 영향을 미치는 것으로 나타났다: 2세 0.253 (95% 유의수준(CI): 0.050, 0.456), 4세 0.243 (95% CI: 0.030, 0.455), 6세 0.251 (95% CI: 0.030, 0.472), 8세 0.322 (95% CI: 0.034, 0.610). 성별에 따라 층화분석했을 경우 남아에서는 cg19196862의 메틸레이션에 따른 BMI Z-score의 변화가 유의하지 않았고 여아에서만 유의하였으며 성별간 차이는 유의했다.

결론: 산모의 비스페놀 A 노출은 자녀의 혈중 *IGF2R* 유전자의 메틸레이션에 영향을 줄 가능성이 있으며 이 영향은 6세가 아닌 2세에서 나타나 자녀가 더 어릴 때 후성유전학적 영향을 미치는 것으로 보인다. 출생 후 비스페놀 A는 594개의 CpG site에서 DNA 메틸레이션에 영향을 주지 않아 출생 전 노출이 더 중요함을 시사한다. 또한 2세 소아의 *IGF2R* 유전자의 메틸레이션 변화는 4세, 6세, 8세까지 지속적으로 체질량지수에 영향을 미쳐 영유아에서 후성유전학적 변화가 학령전기 및 학령기까지 체질량지수에 영향을 미칠 수 있음을 시사한다.

.....

주요어 : 비스페놀 A, 후성유전학, DNA 메틸레이션, 소아, 비만
학 번 : 2018-36285

Supplementary Table 1. List of 594 CpG sites

No.	CpG site	UCSC RefGene Name	UCSC RefGene Group	Relation to UCSC CpG Island	SNP distance†	Minor allele frequency‡	Study
1	cg00033213	<i>TOP1MT</i>	Body	Island	43	2E-04	Huang et al, 2015
2	cg00049616	<i>CLYBL</i>	Body	N_Shelf	6	2E-04	Rzehak et al, 2017
3	cg00094412	<i>GABBR1</i>	Body	N_Shelf	51	1E-03	Wahl et al, 2017
4	cg00119053			N_Shore	28	2E-04	Rzehak et al, 2017
5	cg00134210	<i>FAM107B</i>	Body	N_Shore			Sayols-Baixeras et al, 2017
6	cg00138407	<i>KLHL18</i>	3'UTR		14	6E-04	Wahl et al, 2017
7	cg00234616	<i>TLX2</i>	TSS1500	Island			Sayols-Baixeras et al, 2017
8	cg00238353	<i>PTPRE</i>	5'UTR				Wahl et al, 2017
9	cg00244001	<i>FAM53B</i>	Body		42	4E-04	Wahl et al, 2017
10	cg00285394	<i>SQLE</i>	Body	S_Shore	2	0.033	Sharp et al, 2017
11	cg00431050	<i>ELOVL3</i>	TSS1500	N_Shore			Wahl et al, 2017
12	cg00510507	<i>ANK3</i>	Body		4	2E-04	Lin et al, 2017
13	cg00526953			N_Shore	18	0.002	Sharp et al, 2015
14	cg00574958	<i>CPT1A</i>	5'UTR	N_Shore	4	2E-04	Aslibekyan et al, 2015
15	cg00577950	<i>PDXK</i>	3'UTR	N_Shore	30	4E-04	Rzehak et al, 2017
16	cg00585790	<i>LIMS1</i>	1stExon				Sayols-Baixeras et al, 2017
17	cg00634542	<i>SLC11A1</i>	Body	N_Shore	49	2E-04	Wahl et al, 2017
18	cg00673344			S_Shore			Wahl et al, 2017
19	cg00682263	<i>MEGF11</i>	3'UTR		50	1E-04	Huang et al, 2015
20	cg00696044				37	6E-04	Huang et al, 2015
21	cg00711896	<i>ZNF48</i>	Body	N_Shore	34	2E-04	Wahl et al, 2017
22	cg00729699	<i>EPB49</i>	5'UTR	S_Shelf	44	6E-04	Sharp et al, 2017
23	cg00851028				26	2E-04	Dhana et al, 2018
24	cg00852675	<i>LOC728743</i>	Body	Island	19	2E-04	Rzehak et al, 2017
25	cg00863378	<i>BBS2</i>	Body	N_Shelf	23	2E-04	Demerath et al, 2015
26	cg00905156	<i>FAM13A</i>	1stExon		17	4E-04	Rzehak et al, 2017
27	cg00968488				51	2E-04	Huang et al, 2015
28	cg00973118	<i>AXINI</i>	Body	N_Shore	29	2E-04	Wahl et al, 2017
29	cg01101459				3	2E-04	Wahl et al, 2017
30	cg01115923	<i>KIFC3</i>	Body	N_Shore	38	2E-04	Campanella et al, 2018
31	cg01172150			S_Shore	12	0.005	Sayols-Baixeras et al, 2017
32	cg01188578	<i>HADHA</i>	Body	N_Shelf	41	2E-04	Huang et al, 2015
33	cg01243823	<i>NOD2</i>	Body		30	2E-04	Wahl et al, 2017
34	cg01338599	<i>TM9SF4</i>	1stExon		2	0.001	Rzehak et al, 2017
35	cg01363869	<i>TRIM39</i>	Body	N_Shelf	29	2E-04	Rzehak et al, 2017
36	cg01385356	<i>USP36</i>	TSS1500	Island			Huang et al, 2015

37	cg01428678	<i>GPHN</i>	TSS200	N_Shore			Sharp et al, 2017
38	cg01462036	<i>TBL3</i>	Body	S_Shore	7	2E-04	Rzehak et al, 2017
39	cg01517690				6	0.003	Sharp et al, 2017
40	cg01538605			N_Shore	23	0.011	Campanella et al, 2018
41	cg01565985	<i>CHD5</i>	Body		37	8E-04	Rzehak et al, 2017
42	cg01706498	<i>KLHL6</i>	Body		51	6E-04	Rzehak et al, 2017
43	cg01806722	<i>MAML2</i>	Body				Rzehak et al, 2017
44	cg01840740	<i>AIRE</i>	TSS1500	N_Shore			Rzehak et al, 2017
45	cg01936370			Island			Rzehak et al, 2017
46	cg01963618	<i>LOC285768</i>	TSS1500		16	0.001	Sharp et al, 2017
47	cg01965476	<i>PAK6</i>	5'UTR	N_Shore			Rzehak et al, 2017
48	cg01997599	<i>TRPM4</i>	Body	S_Shelf	14	0.001	Huang et al, 2015
49	cg02081925	<i>DOK3</i>	Body	Island	51	3E-04	Rzehak et al, 2017
50	cg02088292						Huang et al, 2015
51	cg02162339	<i>ING5</i>	Body		8	0.002	Rzehak et al, 2017
52	cg02244028	<i>SCN11A</i>	TSS200				Rzehak et al, 2017
53	cg02259997	<i>FGF9</i>	TSS1500	Island	44	0.002	Rzehak et al, 2017
54	cg02286155			N_Shore	21	2E-04	Wahl et al, 2017
55	cg02381820			Island	17	2E-04	Rzehak et al, 2017
56	cg02393428				10	0.013	Rzehak et al, 2017
57	cg02426464	<i>SLC43A2</i>	Body	S_Shelf	2	2E-04	Sayols-Baixeras et al, 2017
58	cg02518775	<i>CNIH2</i>	Body	S_Shore	49	6E-04	Rzehak et al, 2017
59	cg02560388				39	0.008	Wahl et al, 2017
60	cg02650017	<i>PHOSPHO1</i>	Body	Island			Wahl et al, 2017
61	cg02682525	<i>ANKK1</i>	TSS1500	N_Shore			Rzehak et al, 2017
62	cg02695873			N_Shelf	36	0.002	Rzehak et al, 2017
63	cg02716826	<i>SUGTIP1</i>	Body	N_Shore	5	6E-04	Wahl et al, 2017
64	cg02729344			N_Shore			Lin et al, 2017
65	cg02758870	<i>LOC256880</i>	TSS200	Island	27	2E-04	Sharp et al, 2015
66	cg02868338	<i>EXOSC4</i>	TSS1500	N_Shore			Rzehak et al, 2017
67	cg02942594	<i>LOC148189</i>	Body	Island			Rzehak et al, 2017
68	cg02997111	<i>CYP2SI</i>	TSS1500	Island	28	2E-04	Sharp et al, 2015
69	cg03012642				8	1E-03	Rzehak et al, 2017
70	cg03046925	<i>TRIM15</i>	Body		48	2E-04	Sharp et al, 2017
71	cg03050965	<i>SIPRI</i>	Body	S_Shelf	48	4E-04	Wahl et al, 2017
72	cg03159676				22	6E-04	Wahl et al, 2017
73	cg03174228	<i>TTL11</i>	Body	N_Shore	9	2E-04	Rzehak et al, 2017
74	cg03221837				44	0.029	Sharp et al, 2017
75	cg03241388	<i>SIM2</i>	TSS1500	Island			Sharp et al, 2015
76	cg03258665	<i>EPHA2</i>	Body	N_Shelf	28	4E-04	Sharp et al, 2017
77	cg03314158	<i>LOC652276</i>	TSS200	Island	5	0.008	Huang et al, 2015
78	cg03318904	<i>MAP3K7IP1</i>	Body		46	0.002	Wahl et al, 2017
79	cg03327570				7	2E-04	Wahl et al, 2017
80	cg03393889	<i>NTHL1</i>	Body	N_Shelf	49	5E-04	Rzehak et al, 2017

81	cg03508235	<i>JUB</i>	5'UTR	N_Shelf	51	4E-04	Sayols-Baixeras et al, 2017
82	cg03523676	<i>CPNE6</i>	TSS1500		13	0.001	Wahl et al, 2017
83	cg03595286			Island			Sharp et al, 2015
84	cg03615565	<i>FAM65A</i>	Body	Island	40	2E-04	Rzehak et al, 2017
85	cg03619256	<i>ATXN7L1</i>	Body	N_Shore	31	0.002	Campanella et al, 2018
86	cg03719642			Island	20	1E-03	Sharp et al, 2017
87	cg03725309	<i>SARS</i>	Body	S_Shore	19	4E-04	Wahl et al, 2017
88	cg03737815	<i>TPI1</i>	TSS200	Island			Sharp et al, 2015
89	cg03746015	<i>CLEC16A</i>	Body		28	2E-04	Xu et al, 2018
90	cg03854564	<i>WDR81</i>	TSS1500	N_Shore	15	1E-03	Rzehak et al, 2017
91	cg03862225	<i>CTBP2</i>	TSS1500	Island	26	4E-04	Rzehak et al, 2017
92	cg03885055	<i>C1orf144</i>	3'UTR				Wahl et al, 2017
93	cg03957124			S_Shelf	30	2E-04	Wahl et al, 2017
94	cg04027757	<i>POM121LIP</i>	TSS200	Island			Sharp et al, 2017
95	cg04094751	<i>HSPA12B</i>	Body		42	2E-04	Rzehak et al, 2017
96	cg04126866	<i>C10orf99</i>	TSS1500		48	0	Wahl et al, 2017
97	cg04219544	<i>KRT24</i>	TSS200		49	1E-03	Rzehak et al, 2017
98	cg04232128	<i>TMEM173</i>	Body		14	7E-04	Wahl et al, 2017
99	cg04264638	<i>CLOCK</i>	5'UTR	N_Shore	10	8E-04	Sayols-Baixeras et al, 2017
100	cg04292672	<i>MORNI</i>	Body	N_Shelf	31	2E-04	Rzehak et al, 2017
101	cg04456492				37	2E-04	Huang et al, 2015
102	cg04458776	<i>SLC22A6</i>	TSS1500		47	2E-04	Rzehak et al, 2017
103	cg04556432	<i>SETD3</i>	Body				Rzehak et al, 2017
104	cg04577162	<i>RFC2</i>	Body	N_Shore			Wahl et al, 2017
105	cg04583842	<i>BANP</i>	Body	S_Shore	41	0.007	Campanella et al, 2018
106	cg04726013	<i>LHPP</i>	Body		7	0.002	Sayols-Baixeras et al, 2017
107	cg04836151				24	4E-04	Sharp et al, 2017
108	cg04869770	<i>PBX1</i>	Body		33	0.003	Demerath et al, 2015
109	cg04880874	<i>CCNL2</i>	3'UTR	N_Shore			Rzehak et al, 2017
110	cg04894009	<i>PRKDC</i>	Body		10	2E-04	Rzehak et al, 2017
111	cg04927537	<i>LGALS3BP</i>	TSS200		47	0.019	Demerath et al, 2015
112	cg04972348			Island	33	0.008	Sharp et al, 2017
113	cg04979599	<i>AFAP1L1</i>	TSS1500	N_Shore	47	2E-04	Rzehak et al, 2017
114	cg04984663						Rzehak et al, 2017
115	cg05003422	<i>MCOLN3</i>	5'UTR	Island	43	4E-04	Sharp et al, 2015
116	cg05063895			N_Shelf			Wahl et al, 2017
117	cg05086444	<i>VIPR2</i>	Body	Island	5	2E-04	Sharp et al, 2017
118	cg05095590	<i>MAD1L1</i>	Body		38	0.003	Wahl et al, 2017
119	cg05098566	<i>KIAA1949</i>	Body	N_Shelf	13	2E-04	Rzehak et al, 2017
120	cg05113927	<i>UCN</i>	TSS200	Island			Sharp et al, 2017
121	cg05176551				9	2E-04	Wilson et al, 2017

122	cg05233324				36	8E-04	Kvaloy et al, 2018
123	cg05241536	<i>RGS10</i>	Body	N_Shelf	7	2E-04	Sharp et al, 2015
124	cg05304729	<i>MNDA</i>	TSS1500		34	4E-04	Xu et al, 2018
125	cg05338731	<i>RAB36</i>	Body	S_Shore	38	0.002	Huang et al, 2015
126	cg05572003	<i>GRK6</i>	Body	S_Shelf	31	2E-04	Rzehak et al, 2017
127	cg05596468	<i>ARHGEF10</i>	Body		49	2E-04	Rzehak et al, 2017
128	cg05628049				4	0.003	Sayols-Baixeras et al, 2017
129	cg05635274	<i>PRSS21</i>	TSS1500	N_Shore			Sharp et al, 2017
130	cg05648472	<i>PRDM11</i>	Body	N_Shore	44	6E-04	Wahl et al, 2017
131	cg05659486						Sharp et al, 2017
132	cg05720226	<i>ST7</i>	Body		13	4E-04	Wahl et al, 2017
133	cg05809586	<i>KRTAP27-1</i>	1stExon		33	2E-04	Huang et al, 2015
134	cg05837990				11	4E-04	Sharp et al, 2017
135	cg05845030	<i>DCN</i>	5'UTR		2	0.002	Wahl et al, 2017
136	cg05881436			Island	10	0.002	Sharp et al, 2017
137	cg05899984			N_Shore			Dhana et al, 2018
138	cg05918312	<i>PDE1A</i>	Body		4	4E-04	Sayols-Baixeras et al, 2017
139	cg05979433	<i>CUX2</i>	Body				Rzehak et al, 2017
140	cg06007282			Island	40	2E-04	Rzehak et al, 2017
141	cg06019229	<i>KIF2A</i>	TSS1500	Island	7	0.005	Sharp et al, 2015
142	cg06096336	<i>PSMD1</i>	Body		24	4E-04	Dhana et al, 2018
143	cg06173626	<i>ICOSLG</i>	1stExon	Island	18	8E-04	Sharp et al, 2015
144	cg06192883	<i>MYO5C</i>	Body		38	2E-04	Demerath et al, 2015
145	cg06217450			N_Shore	18	0.009	Rzehak et al, 2017
146	cg06322432			N_Shore			Rzehak et al, 2017
147	cg06369443	<i>KCNQ4</i>	Body	N_Shore	6	8E-04	Rzehak et al, 2017
148	cg06372962	<i>ANKRD45</i>	5'UTR	Island	12	2E-04	Sharp et al, 2015
149	cg06376715	<i>TP73</i>	Body	Island	48	2E-04	Rzehak et al, 2017
150	cg06392109	<i>TTC15</i>	Body		40	1E-03	Rzehak et al, 2017
151	cg06399427				19	4E-04	Sharp et al, 2017
152	cg06410191	<i>LVRN</i>	1stExon	Island	24	0.003	Rzehak et al, 2017
153	cg06437396			N_Shore	50	0.02	Rzehak et al, 2017
154	cg06559575	<i>IGFBP6</i>	TSS1500	N_Shore	9	2E-04	Wahl et al, 2017
155	cg06594770	<i>TRIOBP</i>	TSS200		46	4E-04	Rzehak et al, 2017
156	cg06690548	<i>SLC7A11</i>	Body				Wahl et al, 2017
157	cg06721796	<i>DBNDD2</i>	Body	S_Shore	13	2E-04	Sharp et al, 2015
158	cg06734985				45	0.01	Sayols-Baixeras et al, 2017
159	cg06882533				2	4E-04	Rzehak et al, 2017
160	cg06898549			N_Shelf	5	0.004	Wahl et al, 2017
161	cg06940720			S_Shelf	47	2E-04	Xu et al, 2018
162	cg06946797						Demerath et al, 2015
163	cg07021906	<i>SLC7A5</i>	Body		47	0.003	Wahl et al, 2017
164	cg07037944	<i>DAPK2</i>	Body		43	2E-04	Wahl et al, 2017

165	cg07044115				41	8E-04	Huang et al, 2015
166	cg07091220	<i>ZNF827</i>	Body				Huang et al, 2015
167	cg07136133	<i>PRR5L</i>	5'UTR				Demerath et al, 2015
168	cg07217499	<i>CACNA1C</i>	Body		17	2E-04	Sayols-Baixeras et al, 2017
169	cg07226193	<i>SWAP70</i>	1stExon	Island			Sharp et al, 2015
170	cg07268332	<i>AMPD3</i>	TSS200	S_Shelf	18	2E-04	Sharp et al, 2015
171	cg07357021	<i>PRICKLE2</i>	Body		20	2E-04	Sharp et al, 2017
172	cg07504977			N_Shelf	50	0.003	Aslibekyan et al, 2015
173	cg07570055			Island	22	4E-04	Sharp et al, 2015
174	cg07573872	<i>SBNO2</i>	Body	S_Shelf	38	2E-04	Demerath et al, 2015
175	cg07664183	<i>HAUS6</i>	TSS1500	S_Shore	39	2E-04	Rzehak et al, 2017
176	cg07682160	<i>UPFI</i>	Body		30	0.01	Wahl et al, 2017
177	cg07700233			N_Shore			Huang et al, 2015
178	cg07719679	<i>STEAP4</i>	TSS200				Rzehak et al, 2017
179	cg07728579	<i>FSD2</i>	TSS1500	N_Shelf	2	1E-03	Wahl et al, 2017
180	cg07769588	<i>ATG4D</i>	Body	S_Shore			Wahl et al, 2017
181	cg07800670	<i>DST</i>	Body		2	2E-04	Sayols-Baixeras et al, 2017
182	cg07814318	<i>KLF13</i>	Body	S_Shelf	25	2E-04	Demerath et al, 2015
183	cg07822775	<i>PCSK6</i>	Body		19	0.002	Sharp et al, 2017
184	cg07831312	<i>FAM188B</i>	Body		29	2E-04	Rzehak et al, 2017
185	cg07879897			Island	46	8E-04	Huang et al, 2015
186	cg07918509	<i>ICAM2</i>	Body		20	4E-04	Wilson et al, 2017
187	cg07950000	<i>GRIK1</i>	TSS200	S_Shore	22	4E-04	Sayols-Baixeras et al, 2017
188	cg08008403	<i>LHX9</i>	Body	S_Shore			Rzehak et al, 2017
189	cg08120831	<i>LRRC43</i>	5'UTR	S_Shore			Sayols-Baixeras et al, 2017
190	cg08215255				47	2E-04	Sayols-Baixeras et al, 2017
191	cg08222662	<i>ZC3HAV1</i>	TSS1500	S_Shore			Sharp et al, 2015
192	cg08289937				47	0.014	Sharp et al, 2017
193	cg08305942				46	4E-04	Wahl et al, 2017
194	cg08309687						Wahl et al, 2017
195	cg08339192	<i>SIGLEC14</i>	TSS200		5	1E-03	Sharp et al, 2015
196	cg08352032	<i>MARK4</i>	3'UTR	Island	25	2E-04	Rzehak et al, 2017
197	cg08390209	<i>CDKN2BAS</i>	Body	N_Shore	30	4E-04	Lin et al, 2017
198	cg08407524				43	2E-04	Sharp et al, 2017
199	cg08443038	<i>CBFA2T3</i>	5'UTR	Island	46	2E-04	Wahl et al, 2017
200	cg08540100			S_Shelf			Sayols-Baixeras et al, 2017
201	cg08548559	<i>PIK3IP1</i>	Body	N_Shore	43	2E-04	Wahl et al, 2017
202	cg08568550	<i>C11orf16</i>	TSS200		19	0.001	Rzehak et al, 2017
203	cg08648047	<i>C1orf127</i>	Body		11	2E-04	Wahl et al, 2017
204	cg08857797	<i>VPS25</i>	Body		2	0.002	Demerath et al, 2015

205	cg08877257	<i>MAZ</i>	Body	S_Shore	44	4E-04	Sayols-Baixeras et al, 2017
206	cg08927006	<i>HPSE2</i>	Body	N_Shore			Sharp et al, 2015
207	cg08943374				16	2E-04	Rzehak et al, 2017
208	cg08972190	<i>MAD1L1</i>	Body		48	2E-04	Demerath et al, 2015
209	cg09018739	<i>CPNE2</i>	Body		47	2E-04	Xu et al, 2018
210	cg09047573	<i>NME5</i>	5'UTR				Sayols-Baixeras et al, 2017
211	cg09121516	<i>TFAP4</i>	Body	S_Shore	9	1E-03	Rzehak et al, 2017
212	cg09152259			N_Shelf			Wahl et al, 2017
213	cg09196346			N_Shore	47	0.003	Huang et al, 2015
214	cg09204618	<i>TSSK2</i>	TSS1500	N_Shelf	31	4E-04	Rzehak et al, 2017
215	cg09230763	<i>MAP3K6</i>	Body	Island			Sharp et al, 2017
216	cg09243648				29	0.019	Sharp et al, 2017
217	cg09245901				28	2E-04	Rzehak et al, 2017
218	cg09285795			S_Shore	49	2E-04	Sharp et al, 2017
219	cg09308608	<i>CARHSP1</i>	5'UTR	Island	46	2E-04	Sharp et al, 2015
220	cg09423599	<i>ABCB9</i>	Body	Island			Rzehak et al, 2017
221	cg09572125	<i>SYNGAP1</i>	Body		44	6E-04	Sayols-Baixeras et al, 2017
222	cg09613192				38	2E-04	Wahl et al, 2017
223	cg09636756	<i>ATP9B</i>	Body	Island	39	2E-04	Huang et al, 2015
224	cg09664445	<i>KIAA0664</i>	5'UTR	N_Shore	49	2E-04	Demerath et al, 2015
225	cg09712306	<i>AURKA</i>	Body				Huang et al, 2015
226	cg09719956	<i>SNORA1</i>	TSS1500		29	2E-04	Huang et al, 2015
227	cg09777883			N_Shelf	27	0.007	Wahl et al, 2017
228	cg09831562	<i>SOX2OT</i>	TSS1500				Campanella et al, 2018
229	cg09927637	<i>KIAA0664</i>	Body	N_Shore	6	0.021	Rzehak et al, 2017
230	cg09936845	<i>NTRK1</i>	Body		11	2E-04	Rzehak et al, 2017
231	cg09956615	<i>TTYH3</i>	Body	S_Shore	51	2E-04	Sayols-Baixeras et al, 2017
232	cg10044470						Xu et al, 2018
233	cg10054641	<i>TMEM71</i>	TSS200		7	0.003	Huang et al, 2015
234	cg10094443	<i>UGDH</i>	TSS1500	S_Shore	20	0.011	Sayols-Baixeras et al, 2017
235	cg10104810	<i>NOTCH2</i>	1stExon	Island	12	4E-04	Rzehak et al, 2017
236	cg10108042	<i>MAPK8IP3</i>	Body		5	2E-04	Rzehak et al, 2017
237	cg10161743	<i>GRIN2D</i>	Body	N_Shore	2	6E-04	Rzehak et al, 2017
238	cg10179300	<i>TRIO</i>	Body	S_Shelf	2	2E-04	Wahl et al, 2017
239	cg10187674	<i>ABCA5</i>	TSS1500	S_Shore			Sharp et al, 2017
240	cg10384133			N_Shore	23	0.001	Huang et al, 2015
241	cg10413089	<i>CYFIP1</i>	5'UTR		27	2E-04	Rzehak et al, 2017
242	cg10505902	<i>PDE4DIP</i>	3'UTR		9	4E-04	Wahl et al, 2017
243	cg10513161	<i>ABCC5</i>	Body		29	2E-04	Wahl et al, 2017
244	cg10549088				36	2E-04	Wahl et al, 2017
245	cg10601624			S_Shelf			Xu et al, 2018

246	cg10632209	<i>PRDM6</i>	Body	Island	24	2E-04	Rzehak et al, 2017
247	cg10671380	<i>FAH</i>	Body		30	4E-04	Sharp et al, 2015
248	cg10717869	<i>SLC41A1</i>	5'UTR	N_Shore			Wahl et al, 2017
249	cg10746778	<i>SORL1</i>	Body				Huang et al, 2015
250	cg10788371	<i>LRRC32</i>	5'UTR	N_Shore			Rzehak et al, 2017
251	cg10802680	<i>DIABLO</i>	TSS200	S_Shore			Rzehak et al, 2017
252	cg10814005	<i>GPR68</i>	5'UTR		22	4E-04	Wahl et al, 2017
253	cg10861407	<i>FSD1L</i>	TSS1500	N_Shore	10	4E-04	Rzehak et al, 2017
254	cg10922280	<i>DPEP2</i>	TSS1500		40	2E-04	Wahl et al, 2017
255	cg11024682	<i>SREBF1</i>	Body	S_Shelf	27	0.003	Demerath et al, 2015
256	cg11027140	<i>GPR144</i>	TSS1500	Island	42	2E-04	Rzehak et al, 2017
257	cg11080651	<i>ROPNIL</i>	Body	S_Shelf			Wahl et al, 2017
258	cg11156132			S_Shelf			Sharp et al, 2017
259	cg11202345	<i>LGALS3BP</i>	1stExon		28	2E-04	Wahl et al, 2017
260	cg11245333	<i>MOSCI</i>	TSS200	N_Shore	42	2E-04	Rzehak et al, 2017
261	cg11276053	<i>RSPH6A</i>	Body	Island	43	2E-04	Rzehak et al, 2017
262	cg11376147	<i>SLC43A1</i>	Body		35	6E-04	Wahl et al, 2017
263	cg11434973	<i>GUCY2D</i>	Body	Island	42	0.027	Rzehak et al, 2017
264	cg11475880	<i>IQSEC2</i>	Body	Island			Rzehak et al, 2017
265	cg11504355	<i>KIRREL</i>	3'UTR		3	2E-04	Rzehak et al, 2017
266	cg11557901			N_Shore			Huang et al, 2015
267	cg11614585	<i>ANGPT4</i>	TSS200		46	2E-04	Wahl et al, 2017
268	cg11650298				30	0.006	Wahl et al, 2017
269	cg11683482	<i>DMAPI</i>	TSS1500	N_Shore	48	0.001	Kvaloy et al, 2018
270	cg11746362	<i>EP400</i>	Body				Rzehak et al, 2017
271	cg11775828	<i>STK39</i>	Body	N_Shelf	16	0.002	Wilson et al, 2017
272	cg11918450	<i>LTBP1</i>	Body		44	4E-04	Huang et al, 2015
273	cg11927233	<i>NPM1</i>	Body	S_Shore	15	2E-04	Wahl et al, 2017
274	cg11969813	<i>P4HB</i>	Body	N_Shore	11	2E-04	Wahl et al, 2017
275	cg11986743	<i>B4GALT6</i>	3'UTR		44	2E-04	Huang et al, 2015
276	cg12155036			S_Shore			Sharp et al, 2017
277	cg12170787	<i>SBNO2</i>	Body		46	8E-04	Kvaloy et al, 2018
278	cg12213037	<i>SLC35E2</i>	Body	N_Shelf	45	6E-04	Huang et al, 2015
279	cg12342501				42	2E-04	Huang et al, 2015
280	cg12382557	<i>MAEA</i>	3'UTR	N_Shore	48	4E-04	Rzehak et al, 2017
281	cg12466610	<i>MOSC2</i>	Body		40	6E-04	Huang et al, 2015
282	cg12470014			N_Shore	45	8E-04	Rzehak et al, 2017
283	cg12717591	<i>SFMBT2</i>	3'UTR		50	0.04	Rzehak et al, 2017
284	cg12917475	<i>BCL2L2</i>	TSS1500	S_Shelf	42	0.001	Sayols-Baixeras et al, 2017
285	cg12921275	<i>MRPL23</i>	Body	S_Shore	14	8E-04	Rzehak et al, 2017
286	cg12975464	<i>MAML3</i>	TSS200	Island			Sharp et al, 2015
287	cg12978214	<i>NCAMI</i>	Body		51	4E-04	Sayols-Baixeras et al, 2017
288	cg13023210	<i>PAX6</i>	Body	S_Shore	28	2E-04	Rzehak et al, 2017
289	cg13074055				4	4E-04	Kvaloy et al, 2018

290	cg13084458	<i>INTU</i>	TSS1500		30	0.028	Sayols-Baixeras et al, 2017
291	cg13097800				5	2E-04	Wahl et al, 2017
292	cg13123009	<i>LY6G6E</i>	TSS200		24	6E-04	Demerath et al, 2015
293	cg13139542				41	2E-04	Dhana et al, 2018
294	cg13176454				39	2E-04	Sharp et al, 2017
295	cg13247668	<i>MADIL1</i>	TSS200	Island	38	2E-04	Sharp et al, 2015
296	cg13274254	<i>GULP1</i>	5'UTR	Island			Rzehak et al, 2017
297	cg13274938	<i>RARA</i>	Body	N_Shelf	18	8E-04	Wahl et al, 2017
298	cg13298389						Rzehak et al, 2017
299	cg13367929	<i>TSPAN17</i>	Body	S_Shelf	5	4E-04	Rzehak et al, 2017
300	cg13403462	<i>NECAB3</i>	Body	S_Shore			Sharp et al, 2017
301	cg13557773	<i>RASA3</i>	Body	Island	30	0.004	Sharp et al, 2017
302	cg13591783	<i>ANXA1</i>	5'UTR				Wahl et al, 2017
303	cg13641993	<i>FBXO10</i>	5'UTR		29	2E-04	Rzehak et al, 2017
304	cg13708645	<i>KDM2B</i>	Body	N_Shore	13	4E-04	Demerath et al, 2015
305	cg13718870	<i>BRD3</i>	5'UTR	Island	31	2E-04	Rzehak et al, 2017
306	cg13758186						Sharp et al, 2017
307	cg13781414	<i>NACC2</i>	5'UTR		38	0.002	Wahl et al, 2017
308	cg13840239				19	2E-04	Sayols-Baixeras et al, 2017
309	cg13922488	<i>PKN1</i>	Body	S_Shore	48	2E-04	Wahl et al, 2017
310	cg13938098	<i>LAMA4</i>	TSS200	S_Shore	17	2E-04	Rzehak et al, 2017
311	cg14017402				11	0.01	Demerath et al, 2015
312	cg14020176	<i>SLC9A3R1</i>	3'UTR		35	4E-04	Wahl et al, 2017
313	cg14030674	<i>ANK1</i>	Body	N_Shore	43	0.017	Sharp et al, 2017
314	cg14085500	<i>TRIM32</i>	Body		50	4E-04	Rzehak et al, 2017
315	cg14184954				11	4E-04	Sharp et al, 2015
316	cg14204100	<i>KIFC1</i>	Body	N_Shelf			Rzehak et al, 2017
317	cg14229362	<i>TRIB2</i>	TSS200	Island	51	6E-04	Sharp et al, 2015
318	cg14240060				15	4E-04	Rzehak et al, 2017
319	cg14264316				47	2E-04	Wahl et al, 2017
320	cg14270612	<i>ABL1</i>	Body	Island			Rzehak et al, 2017
321	cg14286682	<i>TPD52L3</i>	5'UTR		2	2E-04	Sayols-Baixeras et al, 2017
322	cg14300531						Lin et al, 2017
323	cg14306650	<i>RALGPS1</i>	Body		6	0.002	Huang et al, 2015
324	cg14391016	<i>CCR6</i>	TSS1500		24	2E-04	Rzehak et al, 2017
325	cg14391148	<i>C9orf167</i>	3'UTR	Island	45	0.001	Rzehak et al, 2017
326	cg14401837	<i>NPSR1</i>	TSS1500		38	2E-04	Rzehak et al, 2017
327	cg14434213			S_Shore	44	0.001	Sharp et al, 2017
328	cg14476101	<i>PHGDH</i>	Body	S_Shore	41	0.007	Aslibekyan et al, 2015
329	cg14524775	<i>ARHGEF2</i>	Body	Island			Rzehak et al, 2017
330	cg14524936	<i>SLC6A5</i>	Body		5	6E-04	Huang et al, 2015
331	cg14528056	<i>GBAP1</i>	Body	N_Shelf			Sharp et al, 2017

332	cg14580085				13	2E-04	Huang et al, 2015
333	cg14660676	<i>SQLE</i>	Body	S_Shore			Sharp et al, 2017
334	cg14699734			S_Shore	3	2E-04	Rzehak et al, 2017
335	cg14795409				51	4E-04	Rzehak et al, 2017
336	cg14950834	<i>SPTBN4</i>	TSS1500	Island	8	0.004	Rzehak et al, 2017
337	cg15025089	<i>TAPBP</i>	Body		33	3E-04	Rzehak et al, 2017
338	cg15029475				40	6E-04	Sharp et al, 2017
339	cg15059608	<i>C3orf14</i>	TSS1500	S_Shore	51	0.001	Campanella et al, 2018
340	cg15159104	<i>MAP1A</i>	5'UTR				Dhana et al, 2018
341	cg15240102			Island	45	2E-04	Sharp et al, 2017
342	cg15323828	<i>TMEM63A</i>	Body		15	4E-04	Wahl et al, 2017
343	cg15357118	<i>UGGT1</i>	Body		30	1E-03	Wahl et al, 2017
344	cg15416179	<i>MAP2K3</i>	Body	S_Shore			Dhana et al, 2018
345	cg15439078	<i>MYL3</i>	Body		37	6E-04	Rzehak et al, 2017
346	cg15548101	<i>DGKG</i>	5'UTR	N_Shore	33	2E-04	Sayols-Baixeras et al, 2017
347	cg15557031	<i>MRPL3</i>	TSS200	S_Shore	13	8E-04	Sharp et al, 2015
348	cg15650694	<i>SFRS12</i>	TSS200	Island	33	0.005	Rzehak et al, 2017
349	cg15723028	<i>RIPK2</i>	Body		34	2E-04	Huang et al, 2015
350	cg15857470	<i>SRPK2</i>	Body	S_Shelf	26	6E-04	Sayols-Baixeras et al, 2017
351	cg15871086			N_Shelf	19	8E-04	Demerath et al, 2015
352	cg15903032			Island			Dhana et al, 2018
353	cg15913725	<i>TSSC1</i>	Body	Island	50	2E-04	Sharp et al, 2017
354	cg15914340				3	2E-04	Rzehak et al, 2017
355	cg15941159	<i>GRAMD4</i>	3'UTR	S_Shore	22	0.05	Rzehak et al, 2017
356	cg15971518	<i>PRG2</i>	TSS1500		8	2E-04	Huang et al, 2015
357	cg16003913	<i>MPG</i>	5'UTR	N_Shore	15	8E-04	Sayols-Baixeras et al, 2017
358	cg16151636	<i>NR4A2</i>	TSS1500	Island	31	4E-04	Rzehak et al, 2017
359	cg16163382				2	1E-03	Wahl et al, 2017
360	cg16174341	<i>PFDN5</i>	Body	S_Shore			Rzehak et al, 2017
361	cg16191297	<i>TRAPPC9</i>	Body		46	0.001	Huang et al, 2015
362	cg16246545	<i>PHGDH</i>	Body	S_Shore	50	0.014	Campanella et al, 2018
363	cg16436762	<i>PIWIL4</i>	Body		2	0.006	Huang et al, 2015
364	cg16531903	<i>AICF</i>	TSS1500				Huang et al, 2015
365	cg16578636	<i>PCGF5</i>	Body				Wahl et al, 2017
366	cg16594806				2	0.015	Wahl et al, 2017
367	cg16599983	<i>NOTCH4</i>	Body		49	0.009	Sayols-Baixeras et al, 2017
368	cg16611352	<i>P2RX1</i>	1stExon		40	2E-04	Sayols-Baixeras et al, 2017
369	cg16658008				3	0.022	Rzehak et al, 2017
370	cg16730716	<i>IL32</i>	TSS1500		43	2E-04	Huang et al, 2015
371	cg16755922	<i>FOXK2</i>	Body	S_Shelf	9	2E-04	Xu et al, 2018

372	cg16777782	<i>CDH13</i>	Body		4	8E-04	Rzehak et al, 2017
373	cg16815882	<i>KIAA0319L</i>	Body		34	2E-04	Wahl et al, 2017
374	cg16877087				22	2E-04	Sharp et al, 2017
375	cg16885113				28	2E-04	Huang et al, 2015
376	cg17061862			N_Shelf			Campanella et al, 2018
377	cg17111837	<i>NCRNA00176</i>	Body	Island	21	0.005	Rzehak et al, 2017
378	cg17167536	<i>XKR6</i>	Body		51	4E-04	Rzehak et al, 2017
379	cg17209188	<i>IGF2BP3</i>	Body		47	2E-04	Huang et al, 2015
380	cg17213381	<i>AGPAT1</i>	5'UTR				Huang et al, 2015
381	cg17260706	<i>BCL9L</i>	TSS1500	S_Shore			Wahl et al, 2017
382	cg17272620	<i>LRG1</i>	TSS1500	N_Shelf	9	6E-04	Sharp et al, 2015
383	cg17276103	<i>DDAHI</i>	Body		33	6E-04	Rzehak et al, 2017
384	cg17287155	<i>AHRR</i>	Body		17	2E-04	Aslibekyan et al, 2015
385	cg17287326	<i>AVPII</i>	5'UTR	Island	4	0.002	Rzehak et al, 2017
386	cg17429424	<i>DUSPI</i>	1stExon	Island	3	2E-04	Rzehak et al, 2017
387	cg17459290	<i>LGALS8</i>	Body		40	2E-04	Rzehak et al, 2017
388	cg17478979	<i>ZC3H12D</i>	Body	Island			Sayols-Baixeras et al, 2017
389	cg17514558	<i>PCDHB19P</i>	Body	Island	22	6E-04	Sharp et al, 2017
390	cg17526229			Island	10	0.001	Sayols-Baixeras et al, 2017
391	cg17546649	<i>KIF15</i>	TSS1500	N_Shore	2	2E-04	Sharp et al, 2015
392	cg17560136	<i>EPB49</i>	5'UTR	S_Shore	36	2E-04	Demerath et al, 2015
393	cg17627898	<i>TAOK3</i>	5'UTR		51	1E-03	Huang et al, 2015
394	cg17644856				42	1E-03	Rzehak et al, 2017
395	cg17782974	<i>TRIM8</i>	Body	S_Shelf	9	2E-04	Sharp et al, 2017
396	cg17810765	<i>ANO7</i>	TSS200		12	2E-04	Rzehak et al, 2017
397	cg17822325	<i>SERINC2</i>	Body		17	4E-04	Sayols-Baixeras et al, 2017
398	cg17886162	<i>SMG7</i>	TSS1500	N_Shore			Sharp et al, 2015
399	cg17901584	<i>DHCR24</i>	TSS1500	S_Shore	6	2E-04	Demerath et al, 2015
400	cg17935297	<i>CILP2</i>	Body	Island	18	2E-04	Rzehak et al, 2017
401	cg17936495	<i>SCAMP3</i>	TSS1500	S_Shore	46	4E-04	Rzehak et al, 2017
402	cg17989572	<i>RAB5C</i>	5'UTR	N_Shore			Rzehak et al, 2017
403	cg18030453	<i>LARS2</i>	Body		33	2E-04	Dhana et al, 2018
404	cg18051668			S_Shelf			Rzehak et al, 2017
405	cg18120259	<i>LOC100132354</i>	Body		4	2E-04	Wahl et al, 2017
406	cg18156417	<i>MAP2K2</i>	Body	N_Shore	15	2E-04	Sharp et al, 2017
407	cg18181703	<i>SOCS3</i>	Body	N_Shore	28	0.002	Al Muftah et al, 2016
408	cg18217136	<i>BLCAP</i>	TSS1500	S_Shore	24	0.006	Wahl et al, 2017
409	cg18219562				11	6E-04	Wahl et al, 2017
410	cg18268562	<i>FOXRI</i>	TSS200	Island	3	0.03	Sharp et al, 2017
411	cg18307303	<i>IL12B</i>	1stExon	N_Shore			Demerath et al, 2015

412	cg18330571	<i>EBF3</i>	Body	Island			Sharp et al, 2017
413	cg18499001			Island			Sharp et al, 2017
414	cg18500988			S_Shore			Sayols-Baixeras et al, 2017
415	cg18513344	<i>MUC4</i>	Body				Wahl et al, 2017
416	cg18568872	<i>ZNF710</i>	5'UTR	N_Shelf	51	2E-04	Demerath et al, 2015
417	cg18608055	<i>SBNO2</i>	Body		24	8E-04	Wahl et al, 2017
418	cg18618432			N_Shelf	36	6E-04	Huang et al, 2015
419	cg18649745	<i>ZNF350</i>	TSS200		23	2E-04	Sharp et al, 2015
420	cg18699524	<i>TBCD</i>	Body	Island	41	2E-04	Rzehak et al, 2017
421	cg18704658			N_Shelf			Rzehak et al, 2017
422	cg18787246	<i>ZNF490</i>	1stExon	Island	39	2E-04	Rzehak et al, 2017
423	cg18862566	<i>RUNX2</i>	Body	S_Shore	3	2E-04	Sayols-Baixeras et al, 2017
424	cg18995031	<i>RASA3</i>	Body	Island	45	0.008	Sharp et al, 2017
425	cg19196862	<i>IGF2R</i>	Body		19	2E-04	Rzehak et al, 2017
426	cg19202292			Island	24	0.004	Rzehak et al, 2017
427	cg19217955	<i>DLG4</i>	TSS1500	S_Shore	23	2E-04	Wahl et al, 2017
428	cg19249811	<i>SVIL</i>	Body		31	6E-04	Campanella et al, 2018
429	cg19274401	<i>PEPD</i>	3'UTR	N_Shore	40	0.002	Rzehak et al, 2017
430	cg19358373			S_Shore	37	2E-04	Rzehak et al, 2017
431	cg19373347				34	0.004	Huang et al, 2015
432	cg19377703				14	0.001	Rzehak et al, 2017
433	cg19382175	<i>PDE6A</i>	TSS1500		47	2E-04	Rzehak et al, 2017
434	cg19419146	<i>STK32A</i>	TSS200	Island	38	2E-04	Rzehak et al, 2017
435	cg19586698	<i>OTUD6B</i>	3'UTR		32	2E-04	Huang et al, 2015
436	cg19589396				17	0.001	Wahl et al, 2017
437	cg19615711				13	2E-04	Rzehak et al, 2017
438	cg19680332	<i>BCO2</i>	TSS200				Sharp et al, 2015
439	cg19695507	<i>BEND7</i>	Body		26	0.024	Wahl et al, 2017
440	cg19699682						Huang et al, 2015
441	cg19750657	<i>UFMI</i>	3'UTR				Wahl et al, 2017
442	cg19762797			N_Shelf	10	8E-04	Sharp et al, 2017
443	cg19881557				50	2E-04	Wahl et al, 2017
444	cg19922435	<i>LOC285419</i>	Body				Rzehak et al, 2017
445	cg19926144	<i>DIP2C</i>	Body		14	2E-04	Rzehak et al, 2017
446	cg19935471	<i>MATN2</i>	3'UTR		23	0.002	Huang et al, 2015
447	cg19936757				10	2E-04	Sayols-Baixeras et al, 2017
448	cg19990182	<i>WDR35</i>	TSS200	Island	43	8E-04	Sharp et al, 2015
449	cg19992450	<i>EIF2C2</i>	Body		45	2E-04	Rzehak et al, 2017
450	cg19998073	<i>ZC3H14</i>	3'UTR		29	6E-04	Wahl et al, 2017
451	cg20117675	<i>DHX16</i>	TSS1500	S_Shore	34	2E-04	Wilson et al, 2017
452	cg20118717	<i>SYNGAPI</i>	Body		16	6E-04	Sayols-Baixeras et al, 2017
453	cg20312012	<i>FERIL5</i>	Body		25	2E-04	Huang et al, 2015

454	cg20586210	<i>BDHI</i>	Body		48	2E-04	Rzehak et al, 2017
455	cg20587336	<i>ARMC1</i>	TSS200	S_Shore	12	2E-04	Sharp et al, 2015
456	cg20594982	<i>AGRN</i>	Body	Island			Sharp et al, 2017
457	cg20722088	<i>DUSP6</i>	3'UTR	N_Shelf			Xu et al, 2018
458	cg20779019	<i>CCNH</i>	Body	Island	32	2E-04	Sharp et al, 2015
459	cg20981127	<i>NR2F6</i>	TSS1500	S_Shore	5	2E-04	Sayols-Baixeras et al, 2017
460	cg21108085	<i>CD82</i>	5'UTR	S_Shelf	2	6E-04	Wahl et al, 2017
461	cg21126338	<i>FARP1</i>	Body		7	0.001	Rzehak et al, 2017
462	cg21186778	<i>RCL1</i>	Body		26	2E-04	Sharp et al, 2017
463	cg21282997	<i>IL18RAP</i>	5'UTR				Wilson et al, 2017
464	cg21307484	<i>IL2RB</i>	TSS1500				Campanella et al, 2018
465	cg21429551	<i>GARS</i>	Body	S_Shore	9	0.002	Wahl et al, 2017
466	cg21445553	<i>GGTLC1</i>	5'UTR	Island	5	0.001	Sharp et al, 2017
467	cg21486834	<i>RHBDF2</i>	Body	S_Shelf	20	2E-04	Wahl et al, 2017
468	cg21525627				8	0.002	Rzehak et al, 2017
469	cg21584983	<i>ECSIT</i>	TSS200	S_Shore	21	2E-04	Rzehak et al, 2017
470	cg21778193			Island	28	0.002	Sharp et al, 2017
471	cg21814615	<i>KNTC1</i>	Body		25	8E-04	Sharp et al, 2017
472	cg21960828	<i>TADA2B</i>	Body	Island	26	0.002	Rzehak et al, 2017
473	cg22000984	<i>IRGM</i>	1stExon		12	4E-04	Huang et al, 2015
474	cg22012981	<i>ACOX2</i>	5'UTR				Wahl et al, 2017
475	cg22078907	<i>USP22</i>	Body		4	2E-04	Rzehak et al, 2017
476	cg22103219	<i>SH2B2</i>	Body	N_Shore	43	0.04	Wahl et al, 2017
477	cg22243918			S_Shore	46	2E-04	Rzehak et al, 2017
478	cg22259293	<i>PLEC1</i>	TSS1500	Island			Sharp et al, 2015
479	cg22264170				40	2E-04	Rzehak et al, 2017
480	cg22318872	<i>GNAL</i>	Body	S_Shore	46	2E-04	Rzehak et al, 2017
481	cg22352078			Island			Sharp et al, 2015
482	cg22373079	<i>SPRED2</i>	1stExon	Island			Sharp et al, 2015
483	cg22383874	<i>CACNA1G</i>	Body		3	4E-04	Lin et al, 2017
484	cg22503047	<i>BAT2</i>	Body	S_Shore			Rzehak et al, 2017
485	cg22534374			S_Shelf			Wahl et al, 2017
486	cg22545168	<i>LAIR1</i>	3'UTR		19	2E-04	Sharp et al, 2017
487	cg22590032	<i>FLT4</i>	Body	S_Shore	7	2E-04	Wahl et al, 2017
488	cg22695339	<i>CHD3</i>	Body	S_Shelf	36	4E-04	Wahl et al, 2017
489	cg22726039	<i>SLC30A6</i>	TSS1500	Island	27	0.001	Rzehak et al, 2017
490	cg22788657				37	4E-04	Sharp et al, 2015
491	cg22820188	<i>LMNA</i>	Body	S_Shore			Sharp et al, 2017
492	cg23032421	<i>IL5RA</i>	5'UTR		6	8E-04	Wahl et al, 2017
493	cg23080818				51	2E-04	Sharp et al, 2017
494	cg23111106						Sharp et al, 2017
495	cg23131355	<i>STAB2</i>	TSS1500		30	2E-04	Sharp et al, 2015
496	cg23166970	<i>MCCC1</i>	TSS1500	S_Shore	51	6E-04	Sharp et al, 2017
497	cg23172671				39	2E-04	Campanella et al,

							2018
498	cg23232188	<i>EAF2</i>	Body	S_Shelf			Wahl et al, 2017
499	cg23371707	<i>C10orf18</i>	TSS200	Island	15	0.013	Rzehak et al, 2017
500	cg23416307	<i>GAK</i>	Body		48	4E-04	Rzehak et al, 2017
501	cg23483886	<i>LPCAT1</i>	Body				Rzehak et al, 2017
502	cg23577562	<i>RGS12</i>	Body		27	2E-04	Rzehak et al, 2017
503	cg23671997	<i>IGDCC4</i>	Body		5	4E-04	Lin et al, 2017
504	cg23679085	<i>AP2M1</i>	5'UTR	Island			Wilson et al, 2017
505	cg23687103	<i>MIIIP</i>	5'UTR	Island	5	2E-04	Rzehak et al, 2017
506	cg23827531	<i>FAM107A</i>	1stExon		3	0.004	Rzehak et al, 2017
507	cg23884217	<i>APBB2</i>	5'UTR		40	6E-04	Sayols-Baixeras et al, 2017
508	cg23892028			N_Shelf	24	8E-04	Huang et al, 2015
509	cg23893346	<i>NOTCH4</i>	Body				Sayols-Baixeras et al, 2017
510	cg23918315	<i>PCDHB3</i>	TSS1500	N_Shelf	47	2E-04	Huang et al, 2015
511	cg23998749			N_Shelf	5	2E-04	Demerath et al, 2015
512	cg24035595	<i>DLGAP2</i>	Body	N_Shelf	17	1E-03	Rzehak et al, 2017
513	cg24067118			N_Shore	14	4E-04	Rzehak et al, 2017
514	cg24074783			Island	44	0.025	Rzehak et al, 2017
515	cg24102266	<i>KIAA1522</i>	Body	Island			Rzehak et al, 2017
516	cg24174557	<i>TMEM49</i>	Body				Wahl et al, 2017
517	cg24217948	<i>SETBP1</i>	5'UTR	S_Shore	46	2E-04	Kvaloy et al, 2018
518	cg24332767	<i>C3orf70</i>	TSS1500	Island	43	1E-03	Rzehak et al, 2017
519	cg24340572						Sayols-Baixeras et al, 2017
520	cg24531955	<i>LOXL2</i>	3'UTR		36	2E-04	Wahl et al, 2017
521	cg24665113	<i>DTNB</i>	Body		2	6E-04	Rzehak et al, 2017
522	cg24673769	<i>CHCHD6</i>	Body	S_Shelf	25	0.005	Rzehak et al, 2017
523	cg24679890	<i>MYO9B</i>	Body		12	2E-04	Wahl et al, 2017
524	cg24751284	<i>APEX1</i>	Body	S_Shore	36	0.001	Rzehak et al, 2017
525	cg24824703	<i>GNAI2</i>	Body	N_Shore	17	0.002	Rzehak et al, 2017
526	cg24824917			N_Shelf			Sayols-Baixeras et al, 2017
527	cg24851651	<i>CCS</i>	Body	S_Shelf			Huang et al, 2015
528	cg24921943	<i>SH3PXD2B</i>	Body		27	0.003	Huang et al, 2015
529	cg25001190	<i>NFIA</i>	Body		42	4E-04	Wahl et al, 2017
530	cg25096107			N_Shelf	48	2E-04	Wahl et al, 2017
531	cg25178683	<i>LGALS3BP</i>	TSS1500		17	4E-04	Demerath et al, 2015
532	cg25185429	<i>ITPRI</i>	Body		46	2E-04	Sharp et al, 2017
533	cg25213362	<i>TMPRSS12</i>	TSS200	Island	2	6E-04	Sharp et al, 2017
534	cg25217710			N_Shelf	7	2E-04	Wahl et al, 2017
535	cg25228737				38	2E-04	Rzehak et al, 2017
536	cg25312229			S_Shore	49	0.019	Sharp et al, 2015
537	cg25349939	<i>GTDC1</i>	Body				Aslibekyan et al, 2015
538	cg25371332						Rzehak et al, 2017

539	cg25432807	<i>POM121L1P</i>	TSS200	Island			Sharp et al, 2017
540	cg25435714				34	0.019	Wahl et al, 2017
541	cg25453122	<i>CHERP</i>	Body	Island	7	2E-04	Rzehak et al, 2017
542	cg25535435	<i>TREML4</i>	TSS1500				Rzehak et al, 2017
543	cg25554998			N_Shore	31	2E-04	Rzehak et al, 2017
544	cg25574849	<i>UBE4A</i>	3'UTR	N_Shelf			Huang et al, 2015
545	cg25639557	<i>FURIN</i>	Body	Island			Rzehak et al, 2017
546	cg25649826	<i>USP22</i>	Body		50	0.008	Wahl et al, 2017
547	cg25685359				19	0.028	Lin et al, 2017
548	cg25734624	<i>CNGA3</i>	Body		47	1E-03	Rzehak et al, 2017
549	cg25799109	<i>ARHGEF3</i>	5'UTR		49	0.026	Campanella et al, 2018
550	cg25830182	<i>NKX6-1</i>	Body	N_Shore			Sharp et al, 2015
551	cg26093966			S_Shelf	36	4E-04	Rzehak et al, 2017
552	cg26140475				22	0.008	Aslibekyan et al, 2015
553	cg26164488						Aslibekyan et al, 2015
554	cg26220185	<i>MADIL1</i>	Body	N_Shore	31	0.002	Sharp et al, 2017
555	cg26261358				25	0.033	Huang et al, 2015
556	cg26284544	<i>SNAPC2</i>	TSS1500	Island			Sharp et al, 2017
557	cg26317405	<i>ATPGD1</i>	Body	Island	27	4E-04	Sharp et al, 2015
558	cg26354221	<i>ADORA2A</i>	TSS1500	S_Shore	2	2E-04	Demerath et al, 2015
559	cg26357885	<i>HSPA2</i>	TSS1500	N_Shore	35	4E-04	Wahl et al, 2017
560	cg26403843	<i>RNF145</i>	Body	N_Shelf			Demerath et al, 2015
561	cg26470501	<i>BCL3</i>	Body	S_Shore	31	2E-04	Campanella et al, 2018
562	cg26542660	<i>CEP135</i>	TSS1500	N_Shore	37	2E-04	Wahl et al, 2017
563	cg26542892	<i>C7orf50</i>	Body	S_Shore	8	2E-04	Huang et al, 2015
564	cg26618041	<i>CILP2</i>	Body	Island	38	2E-04	Rzehak et al, 2017
565	cg26627956	<i>CFLAR</i>	Body		46	0.008	Rzehak et al, 2017
566	cg26642774	<i>IL12RB1</i>	3'UTR		22	2E-04	Huang et al, 2015
567	cg26662102	<i>AJAPI</i>	Body		36	0.006	Rzehak et al, 2017
568	cg26663590			S_Shore	36	1E-03	Wahl et al, 2017
569	cg26666886	<i>ANKRD11</i>	TSS1500	S_Shore			Rzehak et al, 2017
570	cg26680760			N_Shore	45	2E-04	Aslibekyan et al, 2015
571	cg26687842	<i>LOC646982</i>	TSS1500		38	0.016	Wahl et al, 2017
572	cg26710983				25	0.031	Rzehak et al, 2017
573	cg26846943	<i>FYN</i>	5'UTR		49	4E-04	Huang et al, 2015
574	cg26879644				22	1E-03	Rzehak et al, 2017
575	cg26891210	<i>CTSS</i>	3'UTR				Huang et al, 2015
576	cg26899718	<i>SMPD3</i>	Body	N_Shore	49	2E-04	Wilson et al, 2017
577	cg26908356	<i>ABCD3</i>	Body		23	2E-04	Huang et al, 2015
578	cg26916936	<i>LOC399959</i>	Body		24	2E-04	Huang et al, 2015
579	cg26952928	<i>SLC45A4</i>	Body	N_Shore	14	0.001	Wahl et al, 2017

580	cg26995653				27	4E-04	Rzehak et al, 2017
581	cg27038634			N_Shore			Rzehak et al, 2017
582	cg27050612	<i>NFE2L1</i>	Body	N_Shelf	33	4E-04	Wahl et al, 2017
583	cg27087650	<i>BCL3</i>	Body	N_Shore	44	0.001	Wahl et al, 2017
584	cg27102629			N_Shore	43	2E-04	Sharp et al, 2017
585	cg27115863				33	2E-04	Wahl et al, 2017
586	cg27117792				39	2E-04	Wahl et al, 2017
587	cg27179375	<i>POM121LIP</i>	TSS200	Island			Sharp et al, 2017
588	cg27247382	<i>PLEKHM3</i>	3'UTR		48	2E-04	Rzehak et al, 2017
589	cg27267258	<i>ANKRD11</i>	Body		6	2E-04	Rzehak et al, 2017
590	cg27285599	<i>TBCD</i>	Body		26	4E-04	Rzehak et al, 2017
591	cg27388983	<i>ZNF256</i>	TSS200	S_Shore	7	2E-04	Sharp et al, 2015
592	cg27577928			Island			Sayols-Baixeras et al, 2017
593	cg27596172			S_Shelf	15	2E-04	Huang et al, 2015
594	cg27601906	<i>GEM</i>	Body	N_Shelf			Rzehak et al, 2017

Supplementary Table 2. Association between methylation at cg19196862 (*IGF2R*) and BMI and BMI Z-score showing R² (n=59)

Obesity measures	Age (Years)	Overall		Boys†		Girls†		Sex difference (reference: boys)	
		Estimate* (95% CI)	P-value (adjusted R ²)	Estimate (95% CI)	P-value (adjusted R ²)	Estimate (95% CI)	P-value (adjusted R ²)	Estimate	P-value
BMI	2	0.371 (0.070, 0.673)	0.020* (0.3086)	0.343 (-.133, 0.820)	0.165 (-0.010)	0.395 (0.006, 0.785)	0.053 (0.2608)	0.023	0.943
	4	0.280 (-.005, 0.566)	0.061 (0.3304)	0.081 (-.342, 0.504)	0.710 (0.3192)	0.425 (0.051, 0.799)	0.032* (0.219)	0.337	0.259
	6	0.304 (-.120, 0.728)	0.168 (0.2433)	-.283 (-.906, 0.339)	0.378 (0.4114)	0.675 (0.157, 1.193)	0.015* (0.2367)	0.982	0.026*
	8	0.662 (-.055, 1.379)	0.079 (0.2484)	-.144 (-1.16, 0.868)	0.782 (0.5442)	1.245 (0.343, 2.146)	0.010* (0.2535)	1.401	0.053
BMI Z-score	2	0.253 (0.050, 0.456)	0.019* (0.2602)	0.228 (-.092, 0.549)	0.170 (-0.0123)	0.272 (0.011, 0.534)	0.048* (0.2264)	0.025	0.909
	4	0.243 (0.030, 0.455)	0.031* (0.3465)	0.111 (-.204, 0.427)	0.494 (0.3258)	0.339 (0.060, 0.617)	0.022* (0.2514)	0.218	0.328
	6	0.251 (0.030, 0.472)	0.032* (0.2883)	-.041 (-.367, 0.286)	0.809 (0.5813)	0.437 (0.165, 0.709)	0.003* (0.2828)	0.481	0.037*
	8	0.322 (0.034, 0.610)	0.035* (0.2499)	0.018 (-.392, 0.428)	0.932 (0.5162)	0.543 (0.178, 0.908)	0.006* (0.3075)	0.523	0.073

*Adjusted for mother's age at pregnancy, mother's and father's prepregnant BMI, mother's education level, child's sex, preterm birth or not (<37 weeks), underweight at birth or not (<2500g), breastfeeding for ≥6 months or not, child's urinary BPA(ug/creatinine), child's total calorie intake (kcal), and cell type fraction.

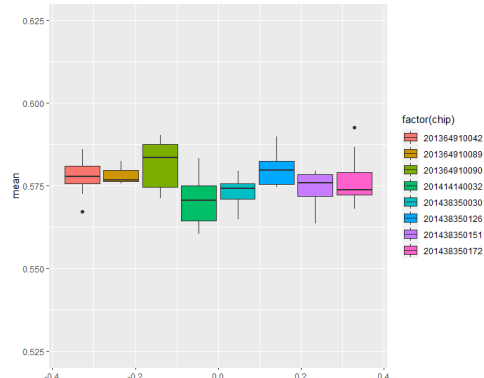
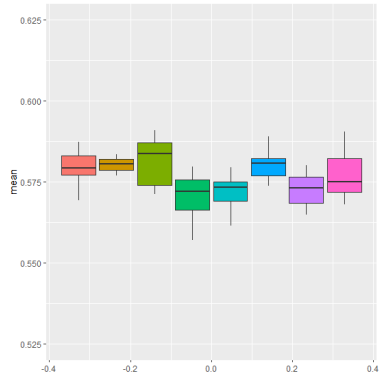
†Estimates for boys and girls were obtained by inserting sex interaction term in the regression analysis.

Supplementary Table 3. Association between methylation level (upper 50 percentile vs. lower 50 percentile) at cg19196862 (*IGF2R*) and BMI and BMI Z-score adjusted for propensity scores showing R² (n=59)

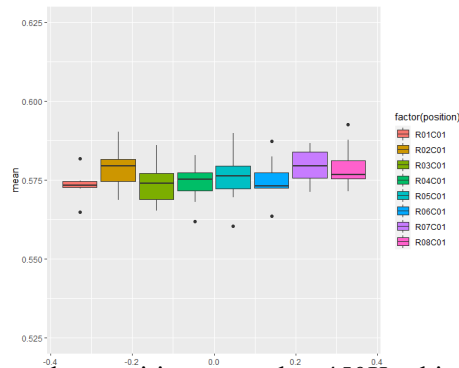
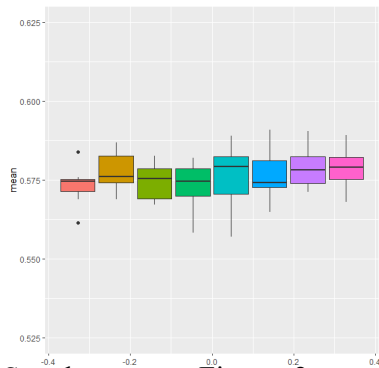
Obesity measures	Age (Years)	Overall		Boys†		Girls†		Sex difference (reference: boys)	
		Estimate* (95% CI)	P-value (adjusted R ²)	Estimate (95% CI)	P-value (adjusted R ²)	Estimate (95% CI)	P-value (adjusted R ²)	Estimate	P-value
BMI	2	0.467 (-0.255, 1.188)	0.201 (0.007)	-0.095 (-1.142, 0.954)	0.854 (-0.063)	1.009 (-0.003, 2.020)	0.051 (0.072)	0.816	0.189
	4	0.584 (-0.076, 1.244)	0.082 (0.021)	0.133 (-0.750, 1.017)	0.758 (-0.729)	1.117 (0.088, 2.146)	0.034* (0.094)	0.661	0.263
	6	0.619 (-0.388, 1.626)	0.223 (-0.003)	-0.181 (-1.733, 1.371)	0.812 (-0.057)	1.413 (0.009, 2.817)	0.049* (0.070)	1.400	0.125
	8	1.306 (-0.183, 2.795)	0.084 (0.055)	-0.179 (-2.628, 2.270)	0.881 (-0.039)	2.623 (0.786, 4.459)	0.007* (0.220)	2.274	0.092
BMI Z-score	2	0.328 (-0.917, 0.393)	0.429 (0.008)	-0.063 (-0.748, 0.623)	0.852 (-0.064)	0.704 (0.025, 1.383)	0.043* (0.082)	0.563	0.172
	4	0.517 (0.0247, 1.010)	0.040* (0.041)	0.211 (-0.453, 0.876)	0.518 (-0.061)	0.892 (0.130, 1.654)	0.023 (0.116)	0.435	0.322
	6	0.483 (-0.947, 0.629)	0.076 (0.022)	0.038 (-0.736, 0.811)	0.621 (-0.071)	0.933 (0.157, 1.709)	0.020 (0.121)	0.763	0.112
	8	0.683 (0.087, 1.281)	0.026* (0.079)	0.075 (-0.890, 1.041)	0.325 (-0.042)	1.230 (0.502, 1.958)	0.002* (0.005)	0.933	0.081

*Adjusted for a propensity score created from mother's age at pregnancy, mother's and father's prepregnant BMI, mother's education level, child's sex, preterm birth or not (<37 weeks), underweight at birth or not (<2500g), breastfeeding for ≥6 months or not, child's urinary BPA(ug/creatinine), child's total calorie intake (kcal), and cell type fraction.

†Estimates for boys and girls were obtained by inserting sex interaction term in the regression analysis.



Supplementary Figure 1. Batch effects by positions on the EPIC chips before (left) and after (right) correction (methylation data at age 2, within the selected 495 CpG sites)



Supplementary Figure 2. Batch effects by positions on the 450K chips before (left) and after (right) correction (methylation at age 6, within the selected 495 CpG sites)

Acknowledgment

First and foremost I am extremely grateful to my esteemed supervisor, Prof. Yun-Chul Hong for his tutelage and patience during my study. I would like to express immense gratitude to Prof. Youn-Hee Lim for her dedicated teaching and support. My gratitude extends to Prof. Sue K. Park for her invaluable mentorship, Prof. Sang Min Park for his priceless advice, and Prof. Ji-Yeob Choi, and Prof. Sanghyuk Bae for their worthy comments. I would like to thank Prof. Young Ah Lee for the inspiring collaboration, and Prof. Choong Ho Shin, Prof. Bung-Nyun Kim, and Prof. Inhyang Kim for providing access to the mother-child cohort. I would like to appreciate Prof. Hans Bisgaard and Prof. Klaus Bønnelykke for their helpful comments and discussion. I would particularly like to thank Kyung-Shin Lee and Jinwoo Cho for their sincere help and support. I would like to appreciate Yumi Choi and Hyun-ji Lee for their assistance in data collection and Hyundong Jin at MacroGen for his technical support.

I would like to appreciate Prof. Youg-Sung Juhn and Prof. Ock Joo Kim for their treasured advice and encouragement for the long period of time. I am also thankful to Prof. Hong Gwan Seo, Prof. Seung-Kwon Myung, Prof. Yeol Kim, Prof. Min Seon Park, Prof. Jin Ho Park, Prof. Ho Chun Choi, and Prof. Jae Moon Yun for their invaluable teaching in medicine. I would like to thank Prof. Belong Cho and Prof. Soong Deok Lee for their kind help and encouragement during the difficult times. I am grateful to my academic inspirer back at University of Toronto from 2000 to 2003: Prof. Arturas Petronis and Prof. Zachary Kaminsky for introducing me to epigenetics and influencing me to pursue a research career. I owe Prof. Randall Pyke for his help and inspiration, which has continuously enriched my ongoing research.

It was a great honor and pleasure to have learned the core of epidemiology and preventive medicine from Prof. Byung-Joo Park, Prof. Jong-koo Lee, Prof. Daehee Kang, Prof. Aesun Shin, Prof. Kyoung-Bok Min, Prof. Joong-Yub Lee, Prof. Seokyoung Hahn, and Prof. Kyoung Nam Kim at the Department of Preventive Medicine, and Prof. Yoon Kim and

Prof. Young Kyung Do at the Department of Health Policy and Management during the coursework and residency. I would also like to appreciate Dr. Mi-jeong Park for the passionate teaching in public health. I would also like to thank Tae-geun Koo, and SeungRan Hong for their help during the residency.

I would also like to thank my lab members and colleagues, Nam-kyung Song, Prof. Chang Woo Han, Woo-Seok Lee, Dong-Wook Lee, Donghee Seo, Yoonyoung Jang, Sungji Moon, Sohyae Lee, and Dongui Hong for a cherished time spent together in the lab and during my residency. Lastly, I am thankful for my friends, especially, Soo Jin Park, and my family, husband, daughter, and parents for their tremendous support and encouragement all through my studies.

This study was partially supported by grants from the Environmental Health Center funded by the Korean Ministry of Environment, an R&D Research program funded by the Ministry of Food and Drug Safety of Korea (#15162MFDS046), and Basic Science Research Program through the National Research Foundation of Korea funded by the Ministry of Education (2018R1D1A1B07043446 and 2018R1D1A1B07049806).